

OPEN

# Extensive Proliferation of a Subset of Differentiated, yet Plastic, Medial Vascular Smooth Muscle Cells Contributes to Neointimal Formation in Mouse Injury and Atherosclerosis Models

Joel Chappell, Jennifer L. Harman, Vagheesh M. Narasimhan, Haixiang Yu, Kirsty Foote, Benjamin D. Simons, Martin R. Bennett, Helle F. Jørgensen

**Rationale:** Vascular smooth muscle cell (VSMC) accumulation is a hallmark of atherosclerosis and vascular injury. However, fundamental aspects of proliferation and the phenotypic changes within individual VSMCs, which underlie vascular disease, remain unresolved. In particular, it is not known whether all VSMCs proliferate and display plasticity or whether individual cells can switch to multiple phenotypes.

**Objective:** To assess whether proliferation and plasticity in disease is a general characteristic of VSMCs or a feature of a subset of cells.

**Methods and Results:** Using multicolor lineage labeling, we demonstrate that VSMCs in injury-induced neointimal lesions and in atherosclerotic plaques are oligoclonal, derived from few expanding cells. Lineage tracing also revealed that the progeny of individual VSMCs contributes to both alpha smooth muscle actin (aSma)-positive fibrous cap and Mac3-expressing macrophage-like plaque core cells. Costaining for phenotypic markers further identified a double-positive aSma+ Mac3+ cell population, which is specific to VSMC-derived plaque cells. In contrast, VSMC-derived cells generating the neointima after vascular injury generally retained the expression of VSMC markers and the upregulation of Mac3 was less pronounced. Monochromatic regions in atherosclerotic plaques and injury-induced neointima did not contain VSMC-derived cells expressing a different fluorescent reporter protein, suggesting that proliferation-independent VSMC migration does not make a major contribution to VSMC accumulation in vascular disease.

**Conclusions:** We demonstrate that extensive proliferation of a low proportion of highly plastic VSMCs results in the observed VSMC accumulation after injury and in atherosclerotic plaques. Therapeutic targeting of these hyperproliferating VSMCs might effectively reduce vascular disease without affecting vascular integrity. (*Circ Res.* 2016;119:1313-1323. DOI: 10.1161/CIRCRESAHA.116.309799.)

**Key Words:** atherosclerosis ■ lineage-tracing ■ macrophages ■ neointima ■ phenotype ■ vascular diseases ■ vascular smooth muscle

Vascular smooth muscle cell (VSMC) accumulation is a hallmark of atherosclerosis,<sup>1</sup> and VSMCs also generate the bulk of the neointima formed after vessel occlusion or injury.<sup>2-4</sup> VSMCs display remarkable phenotypic plasticity *in vitro*,<sup>5</sup> and lineage-tracing experiments have convincingly shown that VSMC phenotypic switching occurs *in vivo*.<sup>3,4,6-9</sup> Healthy, mature VSMCs are quiescent and express contractile genes, such

as alpha smooth muscle actin (aSma) and smooth muscle myosin heavy chain (SMMHC/Myh11). These contractile genes are downregulated when VSMCs undergo phenotypic switching, which result in increased proliferation, migration, and expression of extracellular matrix.<sup>10</sup> Lineage-tracing experiments have demonstrated that VSMC-derived cells not only form the aSma-positive cells in the fibrous cap, which protects from plaque rupture, but also contribute substantially to the generation of the plaque core. Specifically, mouse models of atherosclerosis manifest VSMC-derived cells that lack aSma and the mature VSMC

Editorial, see p 1262  
In This Issue, see p 1255

Original received August 23, 2016; revision received September 13, 2016; accepted September 27, 2016. In August 2016, the average time from submission to first decision for all original research papers submitted to *Circulation Research* was 13.98 days.

From the Cardiovascular Medicine Division, Department of Medicine (J.C., J.L.H., H.Y., K.F., M.R.B., H.F.J.), Cavendish Laboratory, Department of Physics (B.D.S.), The Wellcome Trust/Cancer Research UK Gurdon Institute (B.D.S.), and Wellcome Trust-Medical Research Council Stem Cell Institute (B.D.S.), University of Cambridge, United Kingdom; and The Wellcome Trust Sanger Institute, Hinxton, Cambridge, United Kingdom (V.M.N.).

The online-only Data Supplement is available with this article at <http://circres.ahajournals.org/lookup/suppl/doi:10.1161/CIRCRESAHA.116.309799/-/DC1>.

Correspondence to Helle F. Jørgensen, PhD, ACCE, Level 6, PO Box 110, Addenbrookes' Biomedical Campus, Cambridge CB2 0QQ, United Kingdom. E-mail hfj22@cam.ac.uk

© 2016 The Authors. *Circulation Research* is published on behalf of the American Heart Association, Inc., by Wolters Kluwer Health, Inc. This is an open access article under the terms of the [Creative Commons Attribution](https://creativecommons.org/licenses/by/4.0/) License, which permits use, distribution, and reproduction in any medium, provided that the original work is properly cited.

*Circulation Research* is available at <http://circres.ahajournals.org>

DOI: 10.1161/CIRCRESAHA.116.309799

### Nonstandard Abbreviations and Acronyms

<b>aSma</b>	alpha smooth muscle actin
<b>SMMHC</b>	smooth muscle myosin heavy chain
<b>VSMC</b>	vascular smooth muscle cell

marker SMMHC/Myh11 but instead express genes associated with other cell types, including macrophages (Mac3),<sup>6–9</sup> which may contribute negatively to disease progression. Importantly, this transdifferentiation is also observed in human plaques,<sup>6,8</sup> highlighting the importance of VSMC plasticity in disease.

VSMC migration has also been proposed to play a major contribution to the accumulation of VSMCs in disease, with suggestions that up to 50% of neointimal cells result from migration of nondividing cells after vascular injury.<sup>11,12</sup> Despite extensive investigation of regulators of VSMC phenotypic switching, the proliferation, migration, and plasticity of individual VSMCs in vascular disease, however, remain controversial. In particular, it is unknown whether all, or only a fraction, of VSMCs in major arteries proliferate and display plasticity and whether individual cells can switch to multiple phenotypes or whether these arise from different VSMC subsets.

Here, we report that clonal expansion of a low proportion of mature VSMCs underlies VSMC accumulation after vascular injury and demonstrate that individual VSMCs have the ability to generate plaque cells of different phenotypes. Furthermore, we find that VSMCs within the media underlying atherosclerotic plaques display features of phenotypic switching without contributing to cells within the plaque. Importantly, our data strongly suggest that migration of nonproliferating cells makes a minor contribution to VSMC accumulation in disease.

## Methods

Detailed descriptions of experimental procedures and animals used are provided in the [Online Data Supplement](#).

All animal experiments were approved by the UK Home Office (PPL70/7565) and the local ethics committee and were performed according to the UK Home Office guidelines. The Myh11-CreERT2,<sup>13</sup> Rosa26-Confetti,<sup>14</sup> and ApoE<sup>-/-</sup><sup>15</sup> lines have all been described. For atherosclerosis studies, Myh11-CreERT2/Rosa26-Confetti/ApoE<sup>-/-</sup> animals were injected with tamoxifen at 6 to 8 weeks and were fed a high-fat diet from week 9 until analysis, as described in [Online Data Supplement](#). Tissue was sectioned, immunostained, and cleared before the confocal microscopy analysis as described in the [Online Data Supplement](#). Animals (Myh11-CreERT2/Rosa26-Confetti) undergoing carotid ligation surgery were injected with tamoxifen at 6 to 8 weeks, the left common carotid artery ligated at the bifurcation 1 week after the final tamoxifen injection, and allowed to recover for 28 days post surgery. Whole-mounted tissue was cleared and analyzed by confocal microscopy, followed by cryosectioning, immunostaining, and clearing before being reanalyzed by confocal microscopy.

Confocal microscopy Z-stacks were processed using Imaris software (Bitplane, Zurich, Switzerland). Images displayed are maximal projections of confocal Z-stacks (generated in Imaris) where indicated in figure legends or individual scans (generated in FIJI). Quantification was performed on confocal Z-stacks in Imaris as described in the [Online Data Supplement](#) to ensure correct scoring of staining in individual cells.

## Results

### Multicolor Labeling of VSMCs

To study the proliferation of individual VSMCs in vivo, we combined the inducible Myh11-CreERT2 transgene,<sup>13</sup> which

is specifically expressed in mature VSMCs, with the Rosa26-Confetti multicolor reporter allele (Figure 1A).<sup>14</sup> We induced recombination in healthy animals with a pulse of tamoxifen, which resulted in random labeling of 70% to 95% of VSMCs with 1 of 4 fluorescent proteins (Online Table I). There was a slight bias toward recombination events resulting in expression of red fluorescent protein in 36% of labeled cells, compared with 26% for yellow fluorescent protein, 9% for nuclear green fluorescent protein, and 29% for membrane-bound cyan fluorescent protein (Online Figure I, light gray bars). Importantly, the specific Confetti label is stably transferred to all progeny after VSMC proliferation independent of expression status of the Myh11-CreERT2 transgene and will, therefore, remain expressed after phenotypic switching (Figure 1B). As expected for a tissue with a low proliferative index, the stochastic labeling of elongated VSMCs generated a mosaic pattern (Figure 1C; Online Figure II), which was constant over months in healthy animals. Recombination was specific to VSMCs as demonstrated by the lack of labeling of cells in other

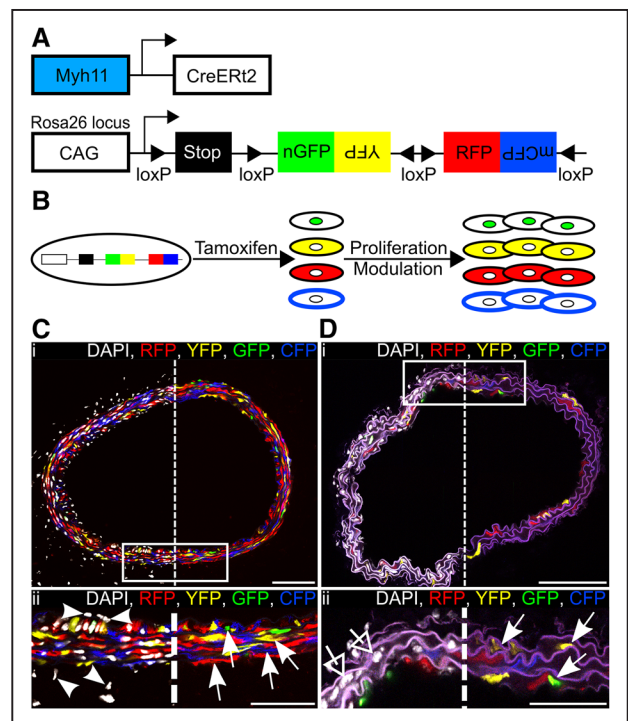


**Figure 1. Efficient and specific multicolor vascular smooth muscle cell (VSMC) labeling in Myh11-CreERT2/Rosa26-Confetti animals.** **A**, Schematic representation of the Myh11-CreERT2 transgene and the Rosa26-Confetti reporter allele. **B**, Schematic representation illustrating tamoxifen-induced recombination at the Rosa26-Confetti locus, resulting in expression of 1 of 4 fluorescent proteins, which are stably propagated independent of Myh11 expression within progeny. **C** and **D**, Carotid artery cross sections from high density-labeled (**C**; 10× 0.1 mg tamoxifen) or low density-labeled (**D**; 1× 0.1 mg tamoxifen) animals; region outlined in (i) is magnified in (ii). Signals for fluorescent proteins are shown with (left) and without (right) nuclear DAPI (4',6-diamidino-2-phenylindole) staining (white). **C**, VSMCs, indicated by arrows in (ii), are labeled with red fluorescent protein (RFP), yellow fluorescent protein (YFP), nuclear (n) green fluorescent protein (GFP), or membrane-associated (m) cyan fluorescent protein (CFP), whereas cells within the adventitia and endothelium, indicated by arrow heads, are unlabeled. In (**D**ii), arrows point to the few labeled VSMCs, and open arrows point to unlabeled VSMCs within the media. Scale bars are 100  $\mu$ m in (i) and 50  $\mu$ m in (ii).

tissues, including adventitia (Online Figure II), bone marrow, peripheral blood, skeletal muscle, lung, and liver (Online Figure III), similar to what was reported in published studies using this transgene with other reporter alleles.<sup>6,8,9,13</sup>

### Clonal Expansion of Few VSMCs in Atherosclerotic Plaques

To study clonal VSMC proliferation in disease, we crossed Myh11-CreERT2/Rosa26-Confetti animals onto an ApoE<sup>-/-</sup> background<sup>15</sup> and induced recombination in 6- to 8-week-old animals before feeding them an atherosclerosis-inducing high-fat diet (21% fat and 0.2% cholesterol) for 16 to 19 weeks (Figure 2A; Online Table II). Accumulation of VSMC-derived cells was assessed by confocal microscopy of arterial cross sections. As expected,<sup>6,8</sup> cells expressing the Confetti reporter, which are derived from Myh11-expressing VSMCs, contributed to both cap and core regions (Figure 2B and 2C; Online Figure IV) and constituted a significant proportion of the total cell number within atherosclerotic lesions. Interestingly, VSMC contribution was similar for the fibrous cap, shoulder, and core regions (Figure 2D). On average, 70% of plaque cells were label-positive (Confetti+) and hence derived from VSMCs, but this ranged from 40% to 90%. Stratification of VSMC contribution according to the vascular region (Online Figure VA) or individual animals (Figure 2E) did not reveal significant differences between regions, suggesting that interplaque variation is not linked to blood lipid level variation or reflects differences in hemodynamic or VSMC developmental origin.<sup>16</sup>

In contrast to the mosaic stochastic labeling observed in the vascular wall, VSMC-derived cells within plaques were found in large monochromatic regions with little intermixing between colors as shown in thick 50- to 100- $\mu$ m sections (Online Figure VI; Online Movie I) or 20- $\mu$ m cryosections (Figure 2B and 2C). Plaques showed substantial variation in color pattern (Online Figure VI), but the frequency of individual colors closely correlated with labeling frequency, demonstrating that there was no bias toward expansion of particular colors (Online Figure I). Quantification of colored regions revealed that most plaques contained 1 or 2 colors (52% and 40%) with a small proportion presenting 3 (6%) or 4 colors (2%; Figure 2F). We compared this observed distribution of colors per plaque (Figure 2F) to the expected distributions in plaques derived from the proliferation of 1, 2, 3, or 4 cells (Figure 2G), which were calculated based on the observed recombination frequency. The disparity from the expected color pattern generated if 3, 4, or more cells proliferate, strongly argues that, typically, a few mature Myh11-expressing VSMCs undergo massive expansion to contribute to plaque formation. However, our analysis clearly shows that plaques in atherosclerotic animals are not exclusively monoclonal, in agreement with recent studies using lineage tracing of SM22a-expressing cells,<sup>7</sup> but in contrast to X-inactivation-based analysis of human lesions.<sup>17</sup>

We confirmed that monochromatic regions arise from clonal expansion of a single cell using lower tamoxifen doses to achieve reduced labeling frequencies. A 10-fold reduction in tamoxifen dose (to 1  $\times$  1 mg/animal) resulted in labeling 40% of VSMCs, which produced many unlabeled plaques

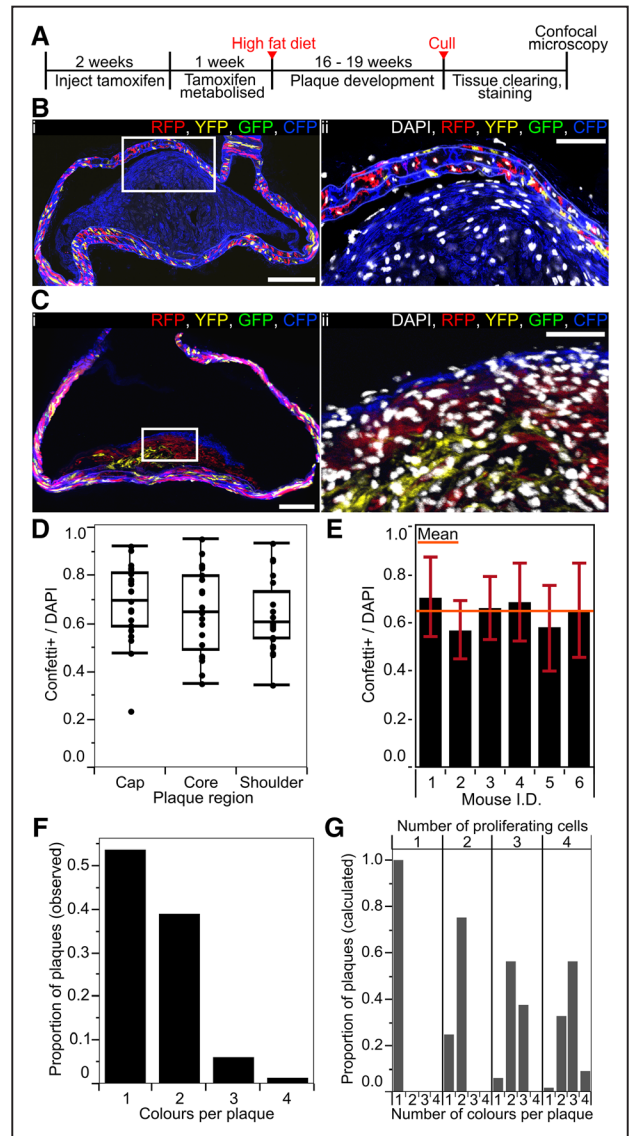


**Figure 2. Vascular smooth muscle cell (VSMC)-derived cells generate oligoclonal atherosclerotic plaques.** **A**, Experimental protocol for the atherosclerosis studies. **B** and **C**, Arterial cryosections from high density-labeled animals (10  $\times$  1 mg tamoxifen) presenting plaques containing VSMC-derived cells of a single color (membrane-associated cyan fluorescent protein [CFP]; **B**) and >1 color (red fluorescent protein [RFP], membrane-associated CFP, and yellow fluorescent protein [YFP]; **C**). The region outlined in (i) is magnified in (ii). Scale bars are 150  $\mu$ m (i) and 50  $\mu$ m (ii). Signals for fluorescent proteins and nuclear DAPI (4',6-diamidino-2-phenylindole; in ii, white) are shown. **D**, Box plot showing the proportion of the total number of cells (DAPI), which express the Confetti reporter (Confetti+) within each plaque region (in 23 plaques from 6 animals). **E**, Bar chart showing the proportion of the total number of cells (DAPI), which express the Confetti reporter (Confetti+) within plaques for 6 individual animals (23 plaques from 6 animals). Mean across all animals is indicated by the orange bar, SD  $\pm$  0.16. **F**, Bar chart showing the number of colors observed per plaque (82 plaques from 16 animals). **G**, Bar chart showing the theoretical distribution of colors per plaque resulting from proliferation of 1, 2, 3, or 4 VSMCs labeled at the recombination frequency observed in high density-labeled animals. All data are from animals labeled at high density (10  $\times$  1 mg tamoxifen).

or plaques, where a single-colored region occupied a large part of the plaque area (Online Figure VII). In addition, we only observed a single monochromatic region within plaques

from 4 animals receiving 0.1 mg tamoxifen (Online Table II). Importantly, the size of the monochromatic regions observed in animals with reduced labeling frequency was comparable to what was found in high density-labeled animals (Online Figure VII). On the basis of these observations, we conclude that monochromatic regions within lesions are generally the progeny of a single cell, signifying that VSMC-derived cells in atherosclerotic lesions are typically formed by the clonal expansion of few VSMCs.

### Generation of Phenotypically Distinct Cells From VSMCs

To assess VSMC plasticity and origin of plaque cells with different phenotypes within monochromatic plaque regions, we stained sequential cryosections for either the VSMC marker aSma or Mac3, which is upregulated as VSMCs adopt a macrophage-like cell type (Figure 3A and 3B). Quantification of staining patterns in different plaque regions showed that aSma+ cells were abundant in the cap and shoulder regions (82% and

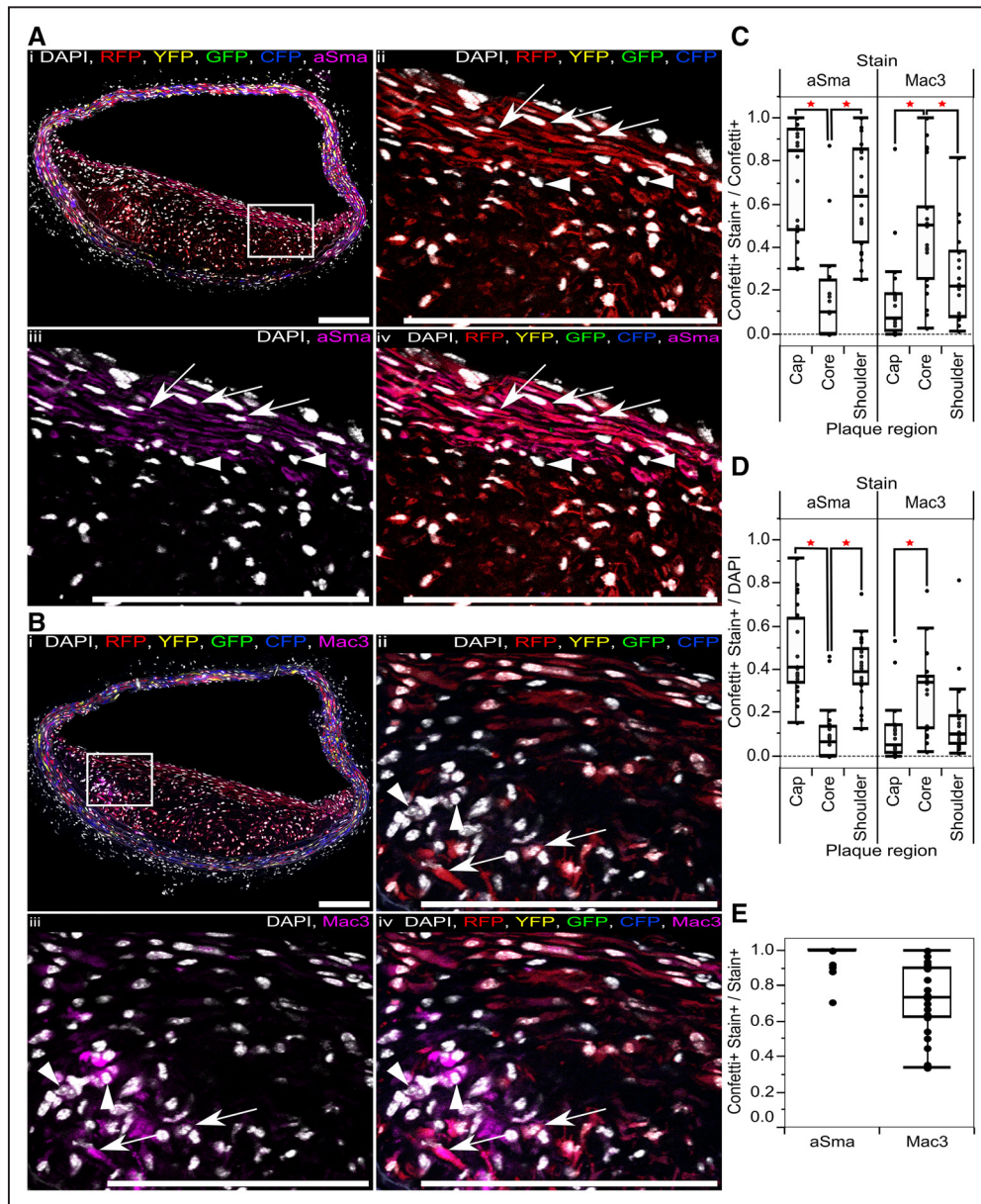


**Figure 3. Progeny of a single vascular smooth muscle cell (VSMC) can adopt multiple phenotypes in disease.** **A and B,** Immunostaining for alpha smooth muscle actin (aSma; **A**) and Mac3 (**B**) of serial cryosections from high density-labeled animal ( $10 \times 1$  mg tamoxifen) containing RFP-expressing VSMC-derived cells. Signals for fluorescent proteins, nuclear DAPI (4',6-diamidino-2-phenylindole; white), aSma (magenta; **A**), and Mac3 (magenta; **B**) are shown as indicated on each image. Regions outlined in (i) are magnified in panels (ii through v), scale bars are  $150 \mu\text{m}$ . **A,** Arrows point to RFP+ aSma+ cells, arrow heads point to RFP- aSma- cells. **B,** Arrows point to RFP+ Mac3+ cells, and arrow heads point to RFP- Mac3+ cells. **C through E,** Box plot showing proportion of cells that express the Confetti reporter and stain positive for either aSma or Mac3 (Confetti+ Stain+), relative to all cells expressing the Confetti reporter (Confetti+; **C**), the total number of cells (DAPI; **D**), or all cells staining positive for aSma or Mac3 markers (Stain+; **E**). A red star indicates a significant difference ( $P < 0.05$ ) determined by a 2-way analysis of variance. Data in (**C through E**) are from 23 plaques from 6 animals. All data are from animals labeled at high density ( $10 \times 1$  mg tamoxifen). CFP indicates cyan fluorescent protein; GFP, green fluorescent protein; RFP, red fluorescent protein; and YFP, yellow fluorescent protein.

62%, respectively, of cells expressing the Confetti reporter), whereas, on average, only 10% of VSMC-derived cells (8% of all cells) in the plaque core expressed aSma (Figure 3C and 3D). Two different single-color lineage-tracing studies reported that 18%<sup>6</sup> or 70%<sup>9</sup> of aSma-expressing cells were VSMC derived, which both lie within the range shown here. The variation possibly reflects the differences between plaque regions, which was not considered in these studies.<sup>6,9</sup> We find that almost all (median 100% and mean 97%) aSma+ cells are derived from Myh11-expressing cells (Figure 3E). This is consistent with the observations that bone marrow-derived cells rarely upregulate VSMC markers, including aSma.<sup>18</sup> The apparent discrepancy with a recent study showing a significant contribution of LysM-Cre-expressing cells to aSma+ plaque cells<sup>9</sup> possibly results from the use of a constitutively active recombinase (rather than tamoxifen inducible) in that study, which might be induced in VSMC-derived plaque cells.

Mac3+ VSMC-derived cells were located predominantly in the core, where they comprised a significant proportion (median 50% of VSMC derived/Confetti+, 34% of all cells, and 73% of Mac3+ cells; Figure 3C through 3E). However, we also observed a variable, but significant number of Mac3-expressing VSMC-derived/Confetti+ cells in the cap and shoulder regions (7% and 22%, respectively). Interplaque variation in staining pattern was not explained by either

vascular region or differences between animals, except for 1 mouse showing significantly lower VSMC contribution to Mac3-expressing cells (Online Figure VB, VC, and VIII). For comparison, previous studies observed that phenotypically modulated VSMCs generate ~30% of all plaque cells<sup>6</sup> and that 12% of plaque cells expressing another macrophage marker CD68<sup>9</sup>, which is consistent with our findings.

### Individual VSMCs Generate Cells Displaying Different Phenotypes

Comparison of Confetti reporter expression with staining patterns for aSma and Mac3 within sequential cryosections revealed that individual clonal monochromatic regions often (27/37 regions in 23 plaques) contain both aSma- and Mac3-expressing cells. This suggests that VSMC-derived plaque cells displaying different phenotype were generated from a single VSMC, implying that individual VSMCs are highly plastic. To test this idea, we scored the position of 127 monochromatic regions in 82 plaques from 16 high density-labeled animals with respect to plaque cap and core (Online Table III). Some monochromatic regions were restricted to a specific sector of a lesion (11% for cap and 13% for core; Figure 4A) and often (>35%) >1 color was observed within either plaque core or cap (Online Figure IXA). However, most monochromatic regions (96/127) spanned both plaque domains (Figure 4A).

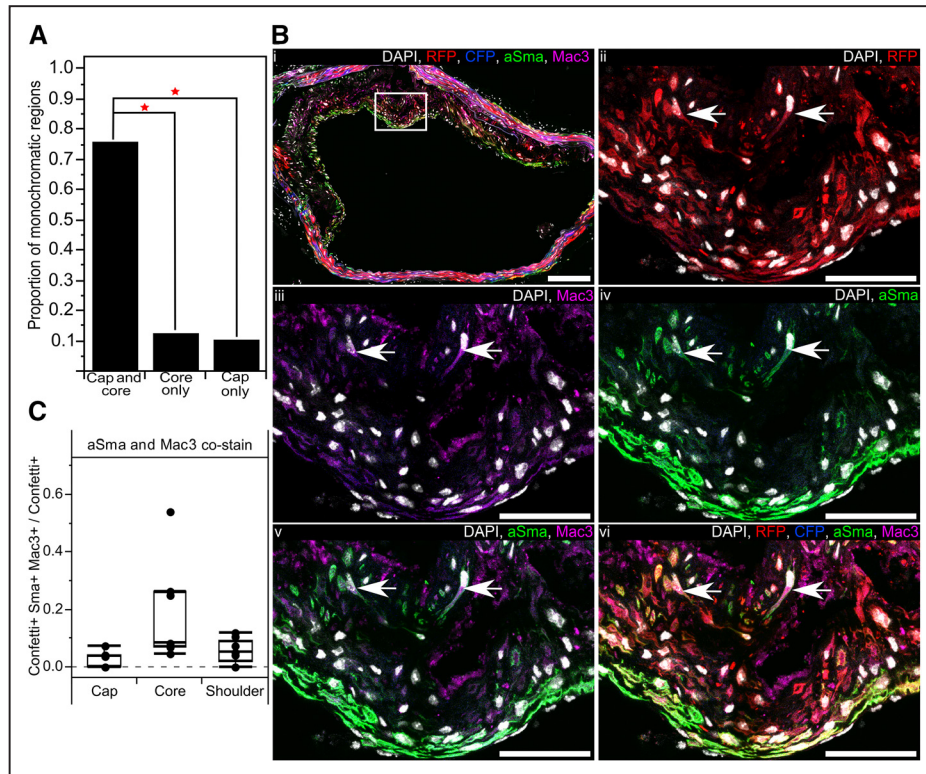


**Figure 4. Progeny of a single vascular smooth muscle cell (VSMC) generates plaque cells with different phenotypes.** **A**, Bar chart showing the proportion of monochromatic regions, which occupy both the cap and core or only a single region within an atherosclerotic plaque (82 plaques from 16 high density-labeled animals). **B**, Arterial cryosection from artery containing red fluorescent protein (RFP)-expressing VSMC-derived cells, costained for alpha smooth muscle actin (aSma) and Mac3. The region outlined in (i) is magnified in (ii through iv). Arrows point to RFP+ Mac3+ aSma+ cells. Scale bars are 150  $\mu$ m (i) and 50  $\mu$ m (ii through vi). Signals for fluorescent proteins, nuclear DAPI (4',6-diamidino-2-phenylindole; white), aSma (green) and Mac3 (magenta) are shown as indicated on each image. **C**, Box plot showing the proportion of cells expressing the Confetti reporter (Confetti+), which co-stain for aSma and Mac3 (Confetti+ aSma+ Mac3+) within different plaque regions (7 plaques from 6 mice). Only red and blue plaques were used for this analysis as the 488 channel was required for aSma imaging. All data are from animals labeled at high density (10 $\times$  1 mg tamoxifen). CFP indicates cyan fluorescent protein.

Importantly, the frequency of such putative bipotent regions was significantly larger than expected by independent chance labeling of 2 proximate unipotent clones ( $\chi^2=228$ ,  $P<0.01$ , 3 degrees of freedom,  $n=96$ ; statistics analysis for each color in [Online Data Supplement](#)). In addition, supporting the conclusion that individual VSMCs can give rise to both fibrous cap and plaque core cells, monochromatic regions in animals with reduced labeling frequency also spanned both cap and core regions (14/17 regions from 14 plaques in 5 animals).

Costaining for aSma and Mac3 demonstrated a low, but consistent, proportion of lineage-labeled plaque cells that express markers of both phenotypes (Figure 4B). Double-positive cells were most abundant in the core and generally located in the region bordering the fibrous cap (Figure 4B and 4C). Interestingly, only 3 of >1100 cells scored costained for aSma and Mac3 without expressing the Confetti reporter, compared with 57 that were positive for aSma, Mac3, and the Confetti reporter, suggesting that coexpression of VSMC and macrophage markers is specific to VSMC-derived plaque cells. Recent single cell analysis similarly suggested coexpression of inflammatory and VSMC markers in VSMC-derived plaque cells, but cell-by-cell data were not presented precluding a direct comparison.<sup>9</sup> Taken together, this analysis demonstrates that individual VSMCs have the ability to generate plaque cells of different phenotypes.

### Plasticity of VSMCs That Do Not Form Monochromatic Regions in the Plaque

In advanced lesions, the medial layer directly underlying plaques was often thickened with loss of the characteristic elongated cell and nucleus morphology of VSMCs (Figure 5A and 5B), indicating that phenotypic changes occur in cells that do not contribute to plaque development. To test this idea, we quantified marker expression in the media underlying plaques compared with the media of regions without visible plaque within the same tissue section. To ensure that the analysis was restricted to nonexpanding cells, we only analyzed medial cells expressing Confetti colors different from those present within the lesion. Relative to medial VSMCs adjacent to the plaque, which were nearly all aSma+ (median 100% and mean 99%), there was a significant reduction in aSma staining in the media under the plaque (25% to 100%, median 68%), suggestive of phenotypic switching of these cells (Figure 5C). This confirms previous reports.<sup>6</sup> Correspondingly, expression of Mac3 was significantly more frequent in Confetti+ cells in the media under the plaque (median 32%) compared to adjacent media where Mac3-positive cells were rarely observed (median 0%; Figure 5C). This demonstrates that changes in VSMC phenotype occur independent of cell expansion but that these changes in medial cells are likely to be a response to the plaque environment and, therefore, a consequence rather than a cause of neointimal growth.

Interestingly, there was a modest, but not significant, reduction in the frequency of cells expressing the Confetti reporter within the media underlying the plaque compared with the adjacent media. Furthermore, whereas virtually no Mac3+ cells were observed in the adjacent media, a significant proportion of Confetti+ Mac3+ cells were found in the media underlying plaques, suggesting an influx of Mac3-expressing

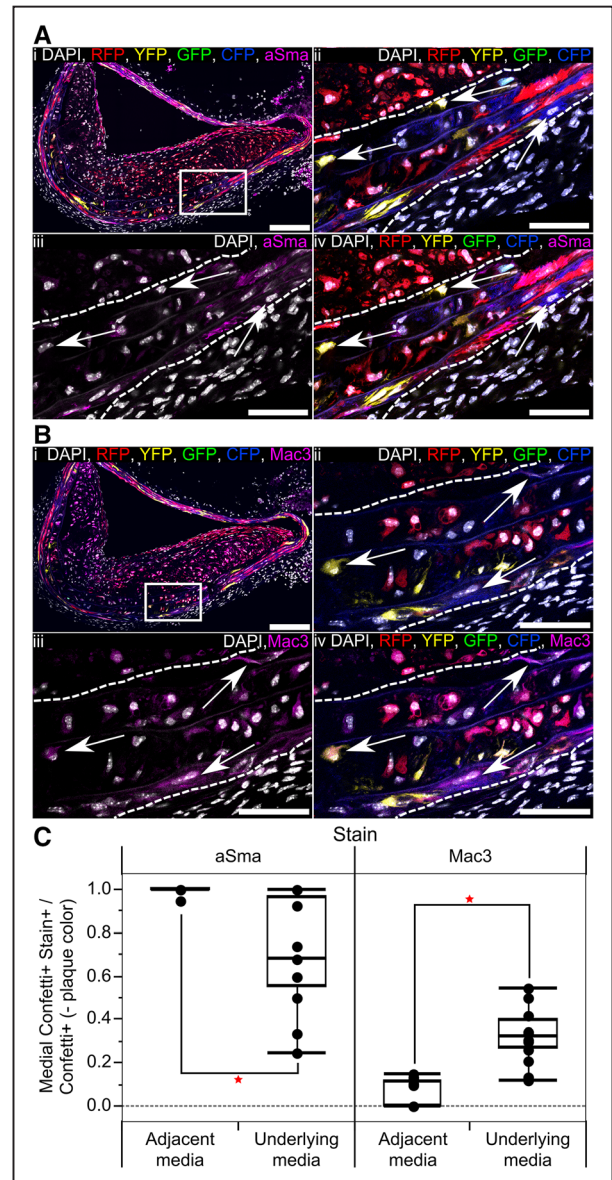


**Figure 5. Vascular smooth muscle cells (VSMCs) within the media directly underlying atherosclerotic plaques undergo phenotypic switching without contributing to the cell mass of the lesion.** **A** and **B**, Serial cryosections from artery of high density-labeled ( $10\times 1$  mg tamoxifen) animal containing a plaque with RFP+ VSMC-derived cells, stained for alpha smooth muscle actin (aSma) (**A**) and Mac3 (**B**). The region outlined in (i) is magnified in (ii through iv), white dotted lines outline the media. Signals for fluorescent proteins, nuclear DAPI (4',6-diamidino-2-phenylindole; white), aSma (magenta; **A**), and Mac3 (magenta; **B**) are shown as indicated on each image. Arrows in (**A**) point to aSma-negative cells within the media, which express the Confetti reporter (excluding RFP-expressing cells). Arrows in (**B**) point to Mac3-positive cells within the media, which express the Confetti reporter (excluding RFP-expressing cells). Scale bars are 150  $\mu$ m in (i) and 50  $\mu$ m in (ii through vi). **C**, Box plot quantifying the proportion of cells expressing the Confetti reporter, which stain positive for aSma or Mac3 (Confetti+ Stain+), relative to all cells expressing Confetti fluorescent proteins not found in the plaque (Confetti+, -plaque color) within the media underlying or adjacent to a plaque (based on 17 plaques from 6 animals). Red stars indicate a significant difference based on a 2-way analysis of variance,  $P<0.05$ . All data are from animals labeled at high density ( $10\times 1$  mg tamoxifen). CFP indicates cyan fluorescent protein; GFP, green fluorescent protein; RFP, red fluorescent protein; and YFP, yellow fluorescent protein.

cells (eg, from the bone marrow or adventitia), accompanying plaque development.

### VSMC Proliferation After Vessel Injury

To test whether the low frequency of proliferating VSMCs in advanced atherosclerotic lesions is a consequence of a low inflammatory signal from the lipid-rich diet or an inherent trait of the VSMC population, we labeled Myh11-CreERT2/Rosa26-Confetti animals at high frequency (10× 1 mg tamoxifen) before ligation of the left carotid artery (Figure 6A), which induces robust and rapid VSMC proliferation.<sup>19</sup> As expected, confocal microscopy analysis of the whole-mounted carotid arteries revealed that VSMCs in the control right carotid artery did not proliferate (Figure 6B). In contrast, the neointima formed in the left carotid artery 28 days after surgery was

composed of large contiguous monochromatic VSMC-derived patches, which occupied a defined volume. This observation suggests that the neointima is formed by clonal proliferation of a small proportion of VSMCs (Figure 6C). Intermingling of colors was only observed where  $\geq 2$  colored patches meet (Figure 6C[iii]). Most animals displayed 2 to 7 colored patches, but this ranged from 1 to 20 (Online Table IV) and correlated with the size of the remodeled area ( $R^2=0.7$ ). Similar to atherosclerotic plaques, patches of all colors were observed after ligation at frequencies comparable to the labeling frequency (Online Figure I), again confirming that recombination does not confer selective advantage to cells expressing a particular fluorescent protein.

Patch size ranged from 48 to >7000 with a median of 435 cells per patch (Figure 6D; Online Table IV). Importantly,

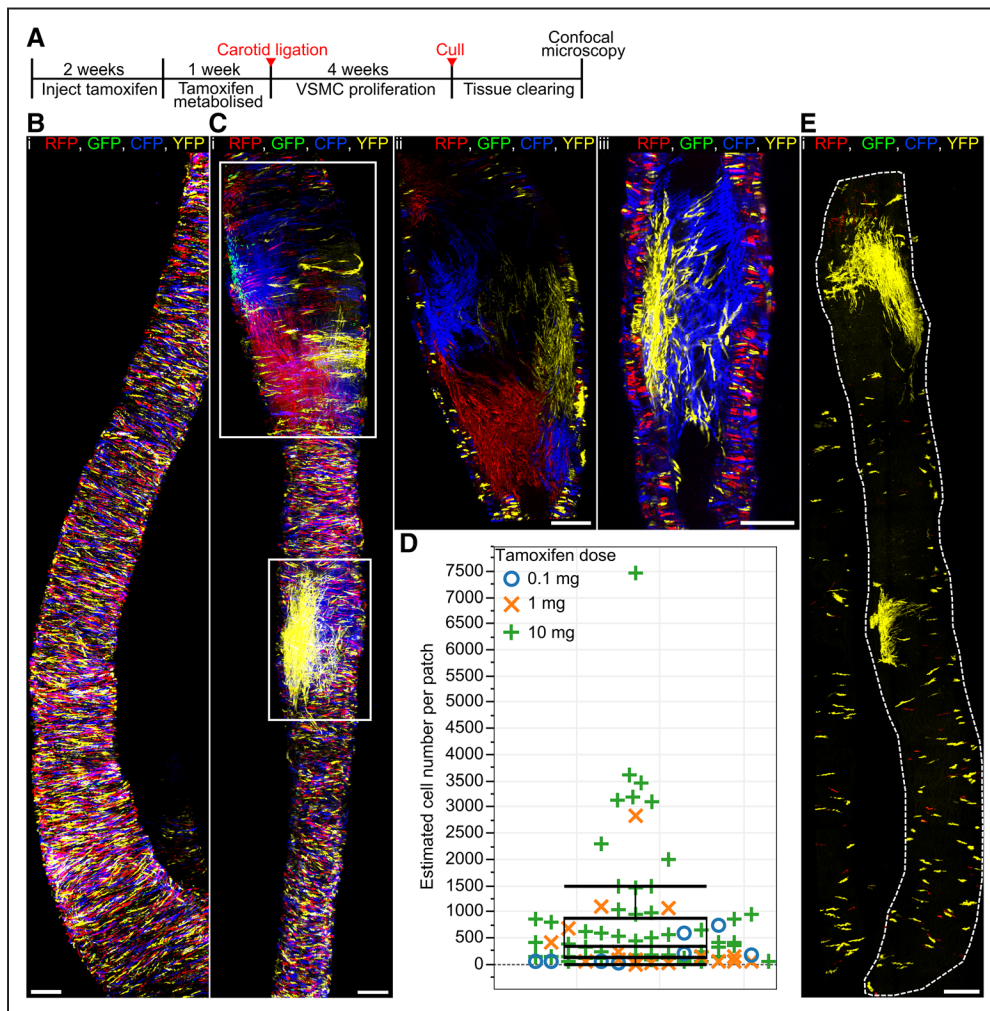


**Figure 6. A subset of vascular smooth muscle cells (VSMCs) proliferate to form the injury-induced neointima.** **A**, Experimental protocol for carotid artery ligation studies. **B** and **C**, Whole-mounted control right carotid artery (**B**) or ligated left carotid artery (**C**) from a high density-labeled animal (10× 1 mg tamoxifen) 28 days post surgery. Maximal projection of confocal Z-stack covering the entire artery is shown in (**B**) and (**C**[i]), whereas (**C**[ii]) and (**C**[iii]) show magnified longitudinal cross section of the regions outlined in (**C**[i]). **D**, Box plot showing the size of individual monochromatic patches. The patch sizes of low (blue circles) and medium density-labeled animals (orange crosses) largely fall within the interquartile range observed in high density-labeled animals (green crosses), strongly suggesting that patches result from clonal expansion of a single cell. Large patches (>1500 cells) might arise from merging of same colored clones. Fifty-two patches from 12 high density-labeled (10× 1 mg), 15 patches from 4 medium density-labeled (1× 1 mg), and 8 patches from 4 low density-labeled animals (1× 0.1 mg) were analyzed. **E**, Maximal confocal Z-stack projection of whole-mounted ligated left carotid artery from a low density-labeled animal (1× 0.1 mg tamoxifen), analyzed 28 days post ligation. Signals for fluorescent proteins are shown. All scale bars are 150  $\mu\text{m}$ . CFP indicates cyan fluorescent protein; GFP, green fluorescent protein; RFP, red fluorescent protein; and YFP, yellow fluorescent protein.

the differences in patch size within the same vessel were on the same scale as interanimal variation, suggesting that this variation is not due to differences associated with the ligation surgery. To assess whether patches resulted from chance merging of independent clones of the same color, we generated low and medium density–labeled animals ( $\approx 1\%$  and  $40\%$  recombination) using reduced tamoxifen doses ( $1 \times 0.1$  and  $1 \times 1$  mg per animal). Remodeled arteries of animals with reduced labeling frequency presented isolated labeled patches comparable to those observed in high density–labeled animals (Figure 6D and 6E). However, median patch size was lower, suggesting that large clones ( $>1500$  cells) could be the result of patch merging. These results demonstrate that a subset of Myh11-expressing cells undergoes multiple rounds of division to generate the neointima after vascular injury. On the basis of a VSMC density of  $\approx 5000$  cells/mm<sup>2</sup>,<sup>20</sup> carotid artery diameter ( $470 \mu\text{m}$ ),<sup>21</sup> and on average  $2.7 \pm 1.0$  patches per mm remodeled artery (Online Table IV), we estimated that  $<0.1\%$  of VSMCs contributed to the formation of the neointima 28 days post ligation. The finding that disease-associated VSMC accumulation results from clonal expansion of a restricted subset of VSMCs that express the mature SMMHC/Myh11 marker in 2 different animal models suggests that this is an inherent feature of this cell population.

### VSMC Plasticity After Vessel Injury

To examine whether clonal proliferation after vascular injury was accompanied by similar phenotypic changes to those observed in atherosclerosis, we immunostained cross sections of arteries (after whole mount imaging) for aSma and Mac3 (Figure 7A through 7C). aSma was expressed in most VSMC-derived neointimal cells 28 days post surgery, although there was a reduction compared with healthy arteries (Online Figure X). In contrast to atherosclerotic plaques, there was little specific localization of aSma+ and aSma– cells expressing the Confetti reporter, although a degree of clustering of aSma-negative cells was observed in some samples (data not shown). We observed an upregulation of Mac3 in a subset of VSMC-derived cells (Figure 7C), but the expression level seemed to be lower than in Mac3+ Confetti+ cells within plaques (Figure 3B). These results demonstrate a clear difference in phenotypic switch–associated gene expression changes between the 2 disease models. We, therefore, tested whether VSMC-derived cells in injury-induced neointima show evidence of an earlier stage of phenotypic switching by staining for SMMHC, which marks fully mature VSMCs and has been reported to be down-regulated early during phenotypic switching.<sup>10</sup> However, the staining pattern for SMMHC was similar to aSma, suggesting that VSMCs in the neointima exist in a largely contractile state (Online Figure XIA).

### Migration of VSMCs in Disease

Interestingly, VSMC-derived neointimal patches were connected to patches expressing the identical Confetti color within the medial layer (Online Figure XII). This suggests that VSMC proliferation initiates in the media and that VSMC progeny then migrate through the elastic laminae, where they continue dividing to form the lesion (Online Figure XIB).<sup>19</sup> Occasional medial patches without a linked neointimal patch

of the same color were observed, indicating that proliferation is not strictly correlated with migration, but that these could be independent events. However, we did not find evidence for significant contribution of migration independent of proliferation to neointima growth, which would generate a mosaic neointima similar to the medial labeling pattern. In particular, coherent neointimal patches did not contain singlet VSMCs expressing other fluorescent proteins (Figure 6C), which would be observed if many cells from the randomly labeled medial wall migrate. This was substantiated by the absence of intermingling of cells expressing different Confetti colors, except at border regions between patches (Figure 6C[iii]).

Similarly, we did not find evidence that migration of non-proliferating cells contributes significantly to atherosclerotic plaque development. Most monochromatic regions formed a coherent structure and few ( $<10\%$ ) displayed intercalation of cells of different colors (for an example of intercalating plaque, Online Figure VIB). Monochromatic VSMC-derived plaque regions did contain interspersed nonlabeled cells (Figure 3A and 3B; arrows heads), which is consistent with the known infiltration of monocytes that contribute to lesion development. As VSMC labeling was not 100% efficient, we cannot rule out that these result from VSMC migration, but this is unlikely as we did not observe plaques that contained VSMC-derived cells expressing another Confetti color within a monochromatic region. We, therefore, suggest that migration of VSMCs independent of proliferation is a minor contribution to VSMC accumulation in vascular disease.

## Discussion

The multicolor lineage–tracing experiments presented here show that extensive proliferation of a small subset of mature, but plastic, VSMCs within major arteries generates neointimal VSMC-derived cells in 2 different vascular disease models. Proliferating VSMCs undergo multiple cell divisions to form large oligoclonal plaques, potentially explaining the replicative exhaustion, telomere shortening, and increased senescence observed in human plaques.<sup>22,23</sup> Consistent with extensive proliferation of VSMC-derived cells, we observed a high proportion of EdU (5-ethynyl-2'-deoxyuridine)-positive Confetti-expressing cells within the neointima of animals that received repeated EdU injections after carotid ligation (Online Figure XIB). Our study correlates with and extends findings from LacZ-lineage tracing of SM22a-positive cells, which marks both mature and immature VSMCs.<sup>7</sup> However, our data in normal adult mice contrast with findings that multiple existing cells proliferate to occlude the vessels of elastin-mutant embryos.<sup>24</sup> This difference is most likely due to lineage labeling of less differentiated embryonic cells (E12.5) in that study<sup>24</sup> compared with adult VSMCs here. The observation that a small fraction of Myh11-expressing VSMCs undergoes clonal expansion in 2 distinct disease models could suggest the existence of specialized cells within arterial walls. This is important as treatments that specifically target the proliferative VSMC population might retain the structural integrity of the artery after injury or in atherosclerosis.

Remarkably, most VSMC clones comprise both macrophage-like cells in the core and aSma-positive cap cells. This



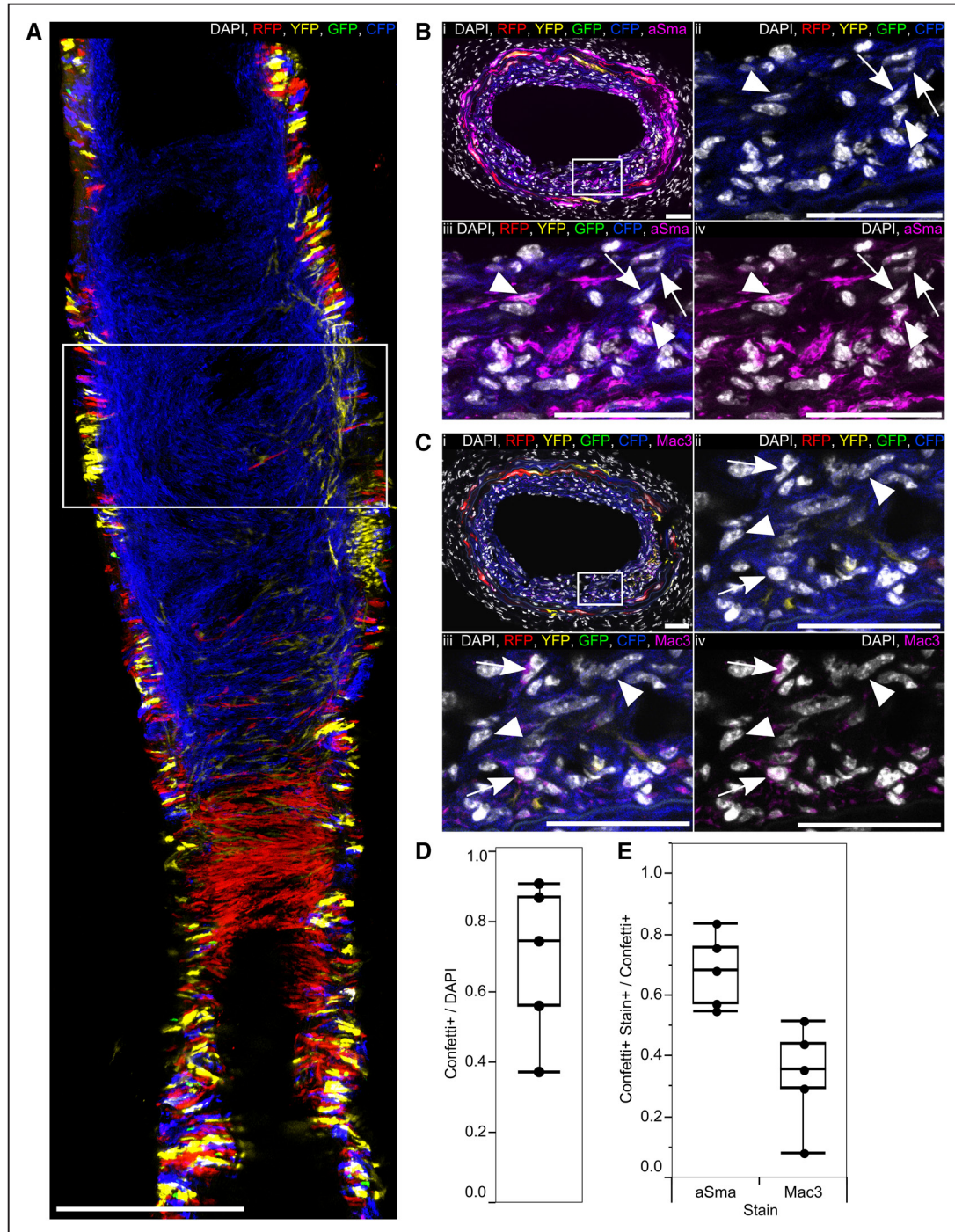


**Figure 7. Injury-induced vascular smooth muscle cell (VSMC)-derived neointima contains few phenotypically switched VSMCs.** **A**, Maximal projection of 3 central scans (7  $\mu\text{m}$  apart) of a confocal Z-stack of whole-mounted ligated left carotid artery from high density-labeled (10 $\times$  1 mg tamoxifen) animal, 28 days post ligation. Scale bar is 300  $\mu\text{m}$ . **B** and **C**, Transverse cryosections from the region outlined in **(A)**, stained for alpha smooth muscle actin (aSma; **B**), or Mac3 (**C**); the region outlined in (i) is magnified in (ii through iv). Arrows point to cells expressing the Confetti reporter (Confetti+) that do not stain for aSma (**B**) and Confetti+ Mac3+ cells (**C**) within the neointima. Arrow heads point to Confetti+ aSma+ cells (**B**) or Confetti+ Mac3- cells (**C**) within the neointima. Scale bars are 50  $\mu\text{m}$ . Signals for fluorescent proteins, nuclear DAPI (4',6-diamidino-2-phenylindole; white), aSma (magenta, **B**), and Mac3 (magenta, **C**) are shown as indicated on each image. **D**, Box plot showing the proportion of all cells (DAPI) within the neointima, which express the Confetti reporter (Confetti+). **E**, Box plot displaying the proportion of Confetti+ neointimal cells that stain positive for aSma or Mac3 (Stain+; based on 5 regions from 4 animals). All data are from high density-labeled (10 $\times$  1 mg tamoxifen) animals. CFP indicates cyan fluorescent protein; GFP, green fluorescent protein; RFP, red fluorescent protein; and YFP, yellow fluorescent protein.

observation establishes that individual VSMCs show phenotypic plasticity as opposed to different VSMC subsets giving rise to different phenotypes. Interestingly, although advanced

atherosclerotic plaques have low proliferative indices,<sup>25</sup> EdU-labeled VSMC-derived cells were observed in both cap and core regions of established plaques, suggesting that cells displaying

different phenotypes undergo cell division within the plaque (Online Figure XIII). Our observation that VSMC-derived cells expressing markers of both phenotypes are found at the border between the aSma-positive cap and the core region, containing macrophage-like VSMC-derived cells, (Figure 4B and 4C) opens the possibility that the VSMC-derived cells could interconvert between different phenotypic states depending on the environmental cues. This is important as it suggests that plaque stabilization could be achieved by therapeutic biasing of proliferating VSMCs toward the protective cap phenotype.

We did not observe differences in the frequency of proliferating VSMCs, their ability to contribute to both cap and core regions, or their bias toward aSma+ or Mac3+ phenotypes between plaques located in the descending aorta compared with the ascending aorta, aortic arch, and carotid arteries (Online Figure IX). This indicates a similar activation frequency and plasticity for VSMCs from different vascular regions, suggesting that there are no overt differences in plasticity of VSMCs generated from different embryonic origins (mesodermal for descending aortic VSMCs versus neural crest for VSMCs within aortic arch and carotid arteries<sup>16</sup>).

Our data suggest that VSMC proliferation and phenotypic switch-associated gene expression changes are not linked. For example, medial cells directly underlying the plaque downregulate aSma and express Mac3 without contributing to plaque mass, and clonally expanded VSMC-derived cells in the injury-induced neointima maintain aSma expression. Furthermore, we show that migration of VSMCs does not make a major contribution to VSMC accumulation in vascular diseases. Our study, therefore, adds *in vivo* single cell evidence supporting a notion that different aspects of VSMC phenotypic switching, including VSMC migration, contractile marker expression, and proliferation, could be regulated independently.

It is not clear why only a small proportion of VSMCs contributed to the observed disease-associated VSMC accumulation, in light of the general response of VSMCs reported after vessel injury.<sup>26</sup> Interestingly, studies using radiolabeled thymidine to measure cell division in pig and rat models of vascular disease suggested that cell proliferation occurs more generally in the media.<sup>27,28</sup> Those studies analyzed animals at earlier time points of disease, as opposed to our analyses of later stages. The apparent difference in the fraction of proliferating medial cells found in those studies and the restricted number of VSMCs we observe contributing to the neointima might, therefore, be due to the differences in time of analysis. For example, clonal selection or cell competition could occur at later time points after a more general response. Alternatively, the different phenotypes could arise from differences between experimental models or the inability to discriminate between VSMCs and infiltrating cells in the previous studies, which did not use lineage labels.<sup>27,28</sup> In any case, it will be interesting to study why the observed phenotypic changes occurring generally in all VSMCs is reversible in most cells but not in a few of the cells. The restriction of migration through the elastic laminae to expanding cells might suggest that the expression of matrix-remodeling factors could be involved. One possibility is that the differential activation of VSMCs we observe is due to the observed heterogeneity between cells in healthy

vessels.<sup>10</sup> Future studies should reveal whether limitation of VSMC contribution to disease-associated cell accumulation in major arteries to a few mature VSMCs that proliferate extensively is associated with somatic mutation,<sup>29</sup> a preselected progenitor pool primed by epigenetic heterogeneity, as suggested for neomuscularization of distal pulmonary arterioles,<sup>30</sup> or due to the rare stochastic activation of an equipotent population.

## Acknowledgments

We thank Jenny Nichols, Doug Winton, Filipe Lourenço, and Crystal McClain for materials and advice; Petko N. Petkov for help with data analysis; Veronique Azuara for comments on the article; and Alison Finigan, Nichola Figg, and Lauren Baker for technical assistance.

## Sources of Funding

This work was funded by the British Heart Foundation grants to H.F. Jørgensen (PG/12/86/29930 and FS/15/38/31516). H.F. Jørgensen and M.R. Bennett acknowledge support from the British Heart Foundation (BHF) Oxbridge Centre of Regenerative Medicine (RM/13/3/30159) and the BHF Cambridge Centre of Research Excellence (RE/13/6/30180). B.D. Simons acknowledges the support of The Wellcome Trust (098357/Z/12/Z). Light microscopy core facilities at Cancer Research UK Cambridge Research Institute, Cambridge Advanced Imaging Centre, and the Wellcome Trust-Medical Research Council, Institute of Metabolic Science, Metabolic Research Laboratories, Imaging core, Wellcome Trust Strategic Award [100574/Z/12/Z] are acknowledged for microscopy and the Cambridge National Institute for Health Research Biomedical Research Centre Cell Phenotyping Hub for flow cytometry. The other authors report no conflicts.

## Disclosures

None.

## References

- Alexander MR, Owens GK. Epigenetic control of smooth muscle cell differentiation and phenotypic switching in vascular development and disease. *Annu Rev Physiol*. 2012;74:13–40. doi: 10.1146/annurev-physiol-012110-142315.
- Nemenoff RA, Horita H, Ostriker AC, Furgeson SB, Simpson PA, VanPutten V, Crossno J, Offermanns S, Weiser-Evans MC. SDF-1 $\alpha$  induction in mature smooth muscle cells by inactivation of PTEN is a critical mediator of exacerbated injury-induced neointima formation. *Arterioscler Thromb Vasc Biol*. 2011;31:1300–1308. doi: 10.1161/ATVBAHA.111.223701.
- Yang P, Hong MS, Fu C, Schmit BM, Su Y, Berceli SA, Jiang Z. Preexisting smooth muscle cells contribute to neointimal cell repopulation at an incidence varying widely among individual lesions. *Surgery*. 2016;159:602–612. doi: 10.1016/j.surg.2015.08.015.
- Herring BP, Hoggatt AM, Burlak C, Offermanns S. Previously differentiated medial vascular smooth muscle cells contribute to neointima formation following vascular injury. *Vasc Cell*. 2014;6:21. doi: 10.1186/2045-824X-6-21.
- Campbell JH, Campbell GR. Smooth muscle phenotypic modulation—a personal experience. *Arterioscler Thromb Vasc Biol*. 2012;32:1784–1789. doi: 10.1161/ATVBAHA.111.243212.
- Shankman LS, Gomez D, Cherepanova OA, Salmon M, Alencar GF, Haskins RM, Swiatlowska P, Newman AA, Greene ES, Straub AC, Isakson B, Randolph GJ, Owens GK. KLF4-dependent phenotypic modulation of smooth muscle cells has a key role in atherosclerotic plaque pathogenesis. *Nat Med*. 2015;21:628–637. doi: 10.1038/nm.3866.
- Feil S, Fehrenbacher B, Lukowski R, Essmann F, Schulze-Osthoff K, Schaller M, Feil R. Transdifferentiation of vascular smooth muscle cells to macrophage-like cells during atherogenesis. *Circ Res*. 2014;115:662–667. doi: 10.1161/CIRCRESAHA.115.304634.
- Gomez D, Shankman LS, Nguyen AT, Owens GK. Detection of histone modifications at specific gene loci in single cells in histological sections. *Nat Methods*. 2013;10:171–177. doi: 10.1038/nmeth.2332.

9. Albarrán-Juárez J, Kaur H, Grimm M, Offermanns S, Wettschureck N. Lineage tracing of cells involved in atherosclerosis. *Atherosclerosis*. 2016;251:445–453. doi: 10.1016/j.atherosclerosis.2016.06.012.
10. Rensen SS, Doevendans PA, van Eys GJ. Regulation and characteristics of vascular smooth muscle cell phenotypic diversity. *Neth Heart J*. 2007;15:100–108.
11. Yu H, Clarke MC, Figg N, Littlewood TD, Bennett MR. Smooth muscle cell apoptosis promotes vessel remodeling and repair via activation of cell migration, proliferation, and collagen synthesis. *Arterioscler Thromb Vasc Biol*. 2011;31:2402–2409. doi: 10.1161/ATVBAHA.111.235622.
12. Clowes AW, Schwartz SM. Significance of quiescent smooth muscle migration in the injured rat carotid artery. *Circ Res*. 1985;56:139–145. doi: 10.1161/01.RES.56.1.139.
13. Wirth A, Benyó Z, Lukasova M, Leutgeb B, Wettschureck N, Gorbey S, Orsy P, Horváth B, Maser-Gluth C, Greiner E, Lemmer B, Schütz G, Gutkind JS, Offermanns S. G12-G13-LARG-mediated signaling in vascular smooth muscle is required for salt-induced hypertension. *Nat Med*. 2008;14:64–68. doi: 10.1038/nm1666.
14. Snippet HJ, van der Flier LG, Sato T, van Es JH, van den Born M, Kroon-Veenboer C, Barker N, Klein AM, van Rheenen J, Simons BD, Clevers H. Intestinal crypt homeostasis results from neutral competition between symmetrically dividing Lgr5 stem cells. *Cell*. 2010;143:134–144. doi: 10.1016/j.cell.2010.09.016.
15. Piedrahita JA, Zhang SH, Hageman JR, Oliver PM, Maeda N. Generation of mice carrying a mutant apolipoprotein E gene inactivated by gene targeting in embryonic stem cells. *Proc Natl Acad Sci USA*. 1992;89:4471–4475. doi: 10.1073/pnas.89.10.4471.
16. Bennett MR, Sinha S, Owens GK. Vascular smooth muscle cells in atherosclerosis. *Circ Res*. 2016;118:692–702. doi: 10.1161/CIRCRESAHA.115.306361.
17. Benditt EP, Benditt JM. Evidence for a monoclonal origin of human atherosclerotic plaques. *Proc Natl Acad Sci USA*. 1973;70:1753–1756.
18. Yu H, Stoneman V, Clarke M, Figg N, Xin HB, Kotlikoff M, Littlewood T, Bennett M. Bone marrow-derived smooth muscle-like cells are infrequent in advanced primary atherosclerotic plaques but promote atherosclerosis. *Arterioscler Thromb Vasc Biol*. 2011;31:1291–1299. doi: 10.1161/ATVBAHA.110.218578.
19. Kumar A, Lindner V. Remodeling with neointima formation in the mouse carotid artery after cessation of blood flow. *Arterioscler Thromb Vasc Biol*. 1997;17:2238–2244. doi: 10.1161/01.ATV.17.10.2238.
20. Clarke MC, Figg N, Maguire JJ, Davenport AP, Goddard M, Littlewood TD, Bennett MR. Apoptosis of vascular smooth muscle cells induces features of plaque vulnerability in atherosclerosis. *Nat Med*. 2006;12:1075–1080. doi: 10.1038/nm1459.
21. Lacolley P, Challande P, Boumaza S, Cohuet G, Laurent S, Boutouyrie P, Grimaud JA, Paulin D, Lamazière JM, Li Z. Mechanical properties and structure of carotid arteries in mice lacking desmin. *Cardiovasc Res*. 2001;51:178–187. doi: 10.1016/S0008-6363(01)00278-4.
22. Gardner SE, Humphry M, Bennett MR, Clarke MC. Senescent vascular smooth muscle cells drive inflammation through an interleukin-1 $\alpha$ -dependent senescence-associated secretory phenotype. *Arterioscler Thromb Vasc Biol*. 2015;35:1963–1974. doi: 10.1161/ATVBAHA.115.305896.
23. Matthews C, Gorenne I, Scott S, Figg N, Kirkpatrick P, Ritchie A, Goddard M, Bennett M. Vascular smooth muscle cells undergo telomere-based senescence in human atherosclerosis: effects of telomerase and oxidative stress. *Circ Res*. 2006;99:156–164. doi: 10.1161/01.RES.0000233315.38086.bc.
24. Misra A, Sheikh AQ, Kumar A, Luo J, Zhang J, Hinton RB, Smoot L, Kaplan P, Urban Z, Qyang Y, Tellides G, Greif DM. Integrin  $\beta$ 3 inhibition is a therapeutic strategy for supraaortic stenosis. *J Exp Med*. 2016;213:451–463. doi: 10.1084/jem.20150688.
25. Lhoták Š, Gyulay G, Cutz JC, Al-Hashimi A, Trigatti BL, Richards CD, Igdoura SA, Steinberg GR, Bramson J, Ask K, Austin RC. Characterization of proliferating lesion-resident cells during all stages of atherosclerotic growth. *J Am Heart Assoc*. 2016;5:e003945. doi: 10.1161/JAHA.116.003945.
26. Kawai-Kowase K, Owens GK. Multiple repressor pathways contribute to phenotypic switching of vascular smooth muscle cells. *Am J Physiol Cell Physiol*. 2007;292:C59–C69. doi: 10.1152/ajpcell.00394.2006.
27. Clowes AW, Reidy MA, Clowes MM. Kinetics of cellular proliferation after arterial injury. I. Smooth muscle growth in the absence of endothelium. *Lab Invest*. 1983;49:327–333.
28. Thomas WA, Florentin RA, Reiner JM, Lee WM, Lee KT. Alterations in population dynamics of arterial smooth muscle cells during atherogenesis. IV. Evidence for a polyclonal origin of hypercholesterolemic diet-induced atherosclerotic lesions in young swine. *Exp Mol Pathol*. 1976;24:244–260.
29. Andreassi MG, Botto N, Colombo MG, Biagini A, Clerico A. Genetic instability and atherosclerosis: can somatic mutations account for the development of cardiovascular diseases? *Environ Mol Mutagen*. 2000;35:265–269. doi: 10.1002/1098-2280.
30. Sheikh AQ, Misra A, Rosas IO, Adams RH, Greif DM. Smooth muscle cell progenitors are primed to muscularize in pulmonary hypertension. *Sci Transl Med*. 2015;7:308ra159. doi: 10.1126/scitranslmed.aaa9712.

## Novelty and Significance

### What Is Known?

- Vascular smooth muscle cell (VSMC) accumulation is a hallmark of vascular disease, including atherosclerosis.
- Mature VSMCs retain phenotypic plasticity, and VSMC-derived cells within atherosclerotic plaques can adopt, among others, a macrophage-like state.

### What New Information Does This Article Contribute?

- A low percentage of VSMCs undergo extensive proliferation to generate monoclonal and oligoclonal neointima after vascular injury and in atherosclerosis.
- Individual VSMCs retain the ability to give rise to VSMC-derived cells within the stabilizing fibrous cap and macrophage-like cells within the plaque core.
- Cell migration independent of proliferation does not make a major contribution to VSMC accumulation in disease models.

Mature VSMCs retain phenotypic plasticity, and VSMC-derived cells constitute the main component of injury-induced neointima and atherosclerotic plaques, but the properties of individual VSMCs are unknown. Here, we show that VSMC accumulation in disease models results from extensive proliferation of a few mature VSMCs. Importantly, our clonal lineage-tracing analysis demonstrates that individual VSMCs can give rise to plaque cells displaying distinct phenotypes. This study suggests that targeting these hyperproliferating cells, or biasing them toward a protective cap phenotype, would efficiently prevent disease progression while maintaining arterial structure.

# Circulation Research

JOURNAL OF THE AMERICAN HEART ASSOCIATION



## Extensive Proliferation of a Subset of Differentiated, yet Plastic, Medial Vascular Smooth Muscle Cells Contributes to Neointimal Formation in Mouse Injury and Atherosclerosis Models

Joel Chappell, Jennifer L. Harman, Vagheesh M. Narasimhan, Haixiang Yu, Kirsty Foote, Benjamin D. Simons, Martin R. Bennett and Helle F. Jørgensen

*Circ Res.* 2016;119:1313-1323; originally published online September 28, 2016;  
doi: 10.1161/CIRCRESAHA.116.309799

*Circulation Research* is published by the American Heart Association, 7272 Greenville Avenue, Dallas, TX 75231  
Copyright © 2016 American Heart Association, Inc. All rights reserved.  
Print ISSN: 0009-7330. Online ISSN: 1524-4571

The online version of this article, along with updated information and services, is located on the  
World Wide Web at:

<http://circres.ahajournals.org/content/119/12/1313>

Free via Open Access

Data Supplement (unedited) at:

<http://circres.ahajournals.org/content/suppl/2016/09/28/CIRCRESAHA.116.309799.DC1.html>

**Permissions:** Requests for permissions to reproduce figures, tables, or portions of articles originally published in *Circulation Research* can be obtained via RightsLink, a service of the Copyright Clearance Center, not the Editorial Office. Once the online version of the published article for which permission is being requested is located, click Request Permissions in the middle column of the Web page under Services. Further information about this process is available in the [Permissions and Rights Question and Answer](#) document.

**Reprints:** Information about reprints can be found online at:  
<http://www.lww.com/reprints>

**Subscriptions:** Information about subscribing to *Circulation Research* is online at:  
<http://circres.ahajournals.org/subscriptions/>

## SUPPLEMENTAL MATERIAL

Supplemental Methods

Supplemental References

Supplemental Legends (Online Figures I-XIII, Online Video I)

Online Tables (I-IV)

Online Figures (I-XIII)

Online Video I (separate file)

### Supplemental Methods

#### ***Animal Experiments***

All animal experiments have been approved by the UK Home Office (PPL70/7565), were performed according to Home Office guidelines and were approved by the local ethics committee. The Myh11-CreERT2<sup>1</sup>, Rosa26-Confetti<sup>2</sup>, ApoE<sup>-/-</sup><sup>3</sup> mouse lines have all been described. Myh11-CreERT2 and ApoE<sup>-/-</sup> were on an inbred C57Bl/6 background (for at least 10 generations), whereas the Rosa26-Confetti allele was on a mixed C57Bl6/BALB/c background prior to crossbreeding. We used experimental animals that had been crossbred between one and six generations (see Online Table II), with no observed difference in the described phenotype. The Myh11-CreERT2 transgene is Y-linked, so all experimental animals in this study were males. Recombination was induced in 6-8 week old animals by intraperitoneal injections of 10x 1 mg (high density-labeling), 1x 1 mg (medium density-labeling) or 1x 0.1 mg (low density-labeling) tamoxifen (Sigma) in corn oil followed by a rest period for at least 1 week before inducing VSMC proliferation by either high fat feeding or carotid ligation surgery. For carotid ligation experiments, Myh11-CreERT2<sup>+</sup>, Rosa26-Confetti<sup>+</sup> animals were anaesthetized with 2.5-3% isoflurane (by inhalation) and given pre-operative analgesic (Temgesic, Buprenorphine). For carotid artery ligation, the left carotid artery was tied just below the bifurcation point. Both the right and left carotid arteries were removed 28 days post-surgery and processed for microscopy. For the atherosclerosis model, Myh11-CreERT2<sup>+</sup>, Rosa26-Confetti<sup>+</sup>, ApoE<sup>-/-</sup> animals were given a high fat diet (Western Rd (p) Product code:829100 SDS, containing 21% fat and 0.2% cholesterol) for 16-19 weeks (except where animals had to be culled prematurely, see Online Table II) starting 1 week after the final tamoxifen injection after which the aorta and carotid arteries were removed.

#### ***Tissue Processing***

Mice were culled by CO<sub>2</sub> asphyxiation and arteries were perfused with PBS. The isolated arteries were dissected free from adipose and connective tissue, fixed (20 minutes at room temperature in 4% (v/w) paraformaldehyde in PBS), washed in PBS, stained with 4',6-diamidino-2-phenylindole (DAPI, 1 µg/ml in PBS, 1h at room temperature) and cleared overnight at 4°C in RapiClear 1.52 (Sunjin lab). Carotid arteries from post-surgery animals were whole mounted in RapiClear 1.52 prior to whole mount confocal microscopy. Post-imaging, carotid arteries were cut transversely into 14 µm thick sections (cryosectioning after overnight equilibration in 30% sucrose/PBS and embedding in TissueTek O.C.T.). The plaque-filled arteries from animals on high fat diet cleared less efficiently and were therefore immediately cut transversely into 50-100 µm (vibratome sectioning after embedding in 4% low melt agarose/ PBS) or 20 µm sections (cryosectioning after overnight equilibration in 30% sucrose/PBS and embedding

in TissueTek O.C.T.). To assess labeling specificity, non-arterial tissue (skeletal muscle, liver, lung) were fixed (20 minutes at room temperature in 4% (v/w) paraformaldehyde in PBS), embedded in 4% low melt agarose and sectioned (100  $\mu\text{m}$ ) using a vibratome. Sections were mounted in RapiClear 1.52 and imaged by confocal microscopy.

### ***Immunostaining***

Serial cryosections were stained for markers of VSMC-derived cell populations or subjected to Haematoxylin/Eosin staining. For immunostaining, sections were briefly rinsed in PBS, permeabilized in 0.3% Triton X-100 in PBS (20 min at room temperature) and incubated for 1h at room temperature in blocking buffer (1% bovine serum albumin, 10% normal goat serum in PBS). Staining with the following primary or isotype control antibodies diluted in blocking buffer was done overnight at 4°C (aSMA - biotin, Abcam, 2.5  $\mu\text{g}/\text{ml}$ , ab125057; aSMA - Alexa Fluor 488, Abcam, 2.5  $\mu\text{g}/\text{ml}$ , ab184675; Mac3 - Alexa Fluor 647, Biolegend, 2.5  $\mu\text{g}/\text{ml}$ , 08511; Myh11, Abcam, 2.5  $\mu\text{g}/\text{ml}$ , ab53219; Mouse IgG2a, k - biotin, Biolegend, 2.5  $\mu\text{g}/\text{ml}$ , 400203; Rat IgG1, k - Alexa Fluor 647, Biolegend, 2.5  $\mu\text{g}/\text{ml}$ , 400418; Rat IgG2a, k - Alexa Fluor 647, Biolegend, 2.5  $\mu\text{g}/\text{ml}$ , 400526; Rabbit IgG, Abcam, 2.5  $\mu\text{g}/\text{ml}$ , ab27478). Sections were then washed 3 times in PBS and incubated with a secondary antibody where necessary (Streptavidin - Alexa Fluor 647, Biolegend, 0.5  $\mu\text{g}/\text{ml}$ , 405237; Goat Anti-Rabbit IgG - Alexa Fluor 647 0.5  $\mu\text{g}/\text{ml}$ , ab150079). Nuclei were stained with DAPI, (1  $\mu\text{g}/\text{ml}$  in PBS, 10 min at room temperature) and mounted in RapiClear 1.52.

### ***Edu administration and detection in carotid ligation and atherosclerosis experiments***

For carotid ligation experiments EdU was dissolved in PBS (5 mg/ml) and injected intraperitoneally (200  $\mu\text{l}$  EdU per injection) starting the day after carotid ligation and every day Monday to Friday following this until they were culled, totalling 19 (200  $\mu\text{l}$ ) injections over 28 days. For atherosclerosis experiments EdU (5 mg/ml) was injected intraperitoneally (300  $\mu\text{l}$ ) three hours before mice were culled at the end of their 16 weeks of high fat diet. Detection was performed using the Click-iT® Plus Edu Alexa Fluor® 657 Imaging kit (Life Tech, C10640) on cryosections according to the manufacturer's instructions.

### ***Imaging and image processing***

Imaging was done using confocal laser scanning microscopy (Leica SP5 or SP8) with laser lines and detectors set for maximal sensitivity without spectral overlap for DAPI (405 laser, 417-508 nm), CFP (458 laser, 454-502 nm), GFP (488 laser, 498-506 nm), YFP (514 laser, 525-560 nm), RFP (561 laser, 565-650 nm) and Alexa Fluor 647 (633 laser, 650-700 nm).

For whole mount samples, a 20x oil objective was used and tile scans of Z-stacks totalling ~400  $\mu\text{m}$  (~6-8  $\mu\text{m}$  between each Z-section) acquired. Cryosections were imaged using a 40x oil objective, tiled Z-stacks typically totalled 20  $\mu\text{m}$  (2- 4  $\mu\text{m}$  separation per Z-section). Vibratome sections were imaged using a 20x oil objective with a Z-stack typically totalling 100  $\mu\text{m}$  (~5  $\mu\text{m}$  between each Z-section). Data was acquired at an optical section resolution of 1024 x 1024 and tiles were stitched using LAS software (Leica).

Imaris 8 software was used for image processing and analysis of whole mount and vibratome samples. Processing includes brightness and contrast adjustments, generation of maximal projections, virtual cross sectioning, animation and surface rendering. For calculation of patch size within whole mount samples, we modelled the surface of individual patches using the surface rendering function within Imaparis. A 'patch' was defined as a large contiguous mass of cells which share the same color and occupy both neointimal and medial compartments of the vessel. To estimate cell number per patch, the surface volume was divided by the volume of an average of 8 individual VSMCs of the same color.

Images are maximal Z-projections (generated in Imaris) where indicated in figure legends or individual scans from a confocal Z-stack (generated in FIJI).

### ***Plaque and neointima scoring***

Plaques were analyzed from three regions within the vasculature; the carotid arteries (CA) comprising the region from where the right and left CA bifurcate to where they meet the aorta; the aortic arch (Arch) comprising the ascending aorta proximal to the aortic root and the arch region; and the descending aorta (DA) comprising the region distal to the Arch region to the bifurcation of the abdominal aorta.

For quantification of imaged cross sections, plaques were separated into three distinct regions; the cap region, which was defined as the organized layer of elongated cells on the inner most surface of the plaque adjacent to the lumen; the core region, which was defined as a disorganized mass of cells towards the centre of a plaque; and the shoulder region, which was defined as the mass of cells within the plaque which are immediately adjacent to the arterial wall on either side of the plaque.

The neointima within carotid ligation samples was defined as the area between the inner elastic lamina (IEL) of the artery wall and the lumen.

Quantification of labeled (Confetti+) and marker positive (Stain+) cells was performed on immunostained cryosections (20  $\mu\text{m}$  for plaque and 14  $\mu\text{m}$  for ligated arteries). Cells within an area of 1  $\text{mm}^2$  were counted for each plaque region and neointima (described above). For almost all plaque regions/neointima (>60%, except where they were too small) two areas were scored for each and the average frequency used. Cell scoring was performed on confocal Z-stacks in Imaris in 3D to evaluate staining within Z-sections below and above the cell of interest. This ensures that counts are made on a cell by cell basis in the high resolution Z-stacks.

T-test and two-way ANOVA test were performed within R (reference<sup>5</sup>) on selected variables to determine significant differences ( $p < 0.05$ ) as indicated in figures.

### ***Calculating theoretical distribution of plaque colors***

To compare the observed distribution of colors per plaque to what would be expected if plaques were generated from proliferation of 1, 2, 3 or 4 cells, we calculated the theoretical distribution as follows. All possible combinations of colored cells were considered (e.g. if 3 cells proliferate there are 64 possible color combinations: red-red-red, red-red-green, red-green-red, red-yellow-blue...). To calculate the probability of each color combination, we applied the known recombination frequency of each color (for example: red-red-red =  $0.34 \times 0.34 \times 0.34$ , red-red-green =  $0.34 \times 0.34 \times 0.07$ , red-green-red =  $0.34 \times 0.07 \times 0.34$ , red-yellow-blue =  $0.34 \times 0.25 \times 0.33$ ...). The frequencies for color combinations of 1, 2, 3 and 4 colors were summed; for example, out of the 64 possible combinations of 3 cells there are 4 yielding one color (red-red-red etc.) with a summed frequency of 0.063, 36x two color combination (summed frequency=0.563), 24x three color combinations (summed frequency=0.375) and 0 x four color combinations. This data is shown in Figure 2G for comparison to the observed distribution shown in Figure 2F.

### ***Statistics analysis of bipotency***

Chi<sup>2</sup> testing was used to assess whether monochromatic regions occupying both cap and core were observed more frequently than what would be expected by chance.

To address the question of bipotency for each Confetti color, we want to compare the observed data against the null hypothesis that “the VSMC cap and core progenitors are unipotent”. The fact that we see some plaques with lineage labeled cells in either the cap or the core but not both suggests that, following activation, at least some of the cells are unipotent. We wish to assess whether they all could be.

To this end, we first assume that contiguously labeled patches in the cap or the core region derive from clonal events. Then, according to the null hypothesis, the probability that a patch in the core will be labeled in color  $c$  is given by

$$P_{\text{core},c} = f q_c$$

where  $f$  denotes the fraction of fluorescently labelled cells, estimated at around 0.8 in the densely labeled sample, and  $q_c$  denotes the relative labeling efficiency of color  $c$ . Similarly, the probability that a patch in the cap is labeled in color  $c$  is given by  $P_{\text{cap},c} = P_{\text{core},c}$ . Then, the chance that we have a clone of color  $c$  in the core but not the cap is given by

$$P_{\text{core},c}(1 - P_{\text{cap},c})$$

(similarly cap but no core), while the probability that both core and cap acquire color  $c$  is given by

$$P_{\text{core},c}P_{\text{cap},c}$$

If we then focus on the ensemble of clones that contain color  $c$  in the cap, the core or both, the relative probabilities must be normalized by the factor

$$P = P_{\text{core},c}(1 - P_{\text{cap},c}) + P_{\text{cap},c}(1 - P_{\text{core},c}) + P_{\text{core},c}P_{\text{cap},c}$$

so that the relative chance of finding a plaque with core labeling of color  $c$

$$r_{\text{core},c} = \frac{P_{\text{core},c}(1 - P_{\text{cap},c})}{P}$$

which is equal to  $r_{\text{cap},c}$ , while the relative chance of finding both labeled in color  $c$  is given by

$$r_{\text{both},c} = P_{\text{core},c}P_{\text{cap},c}/P$$

Finally, for an ensemble of clonal events, we expect that the statistical error on the measured fractions should become defined by the standard error of the mean, given by

$$(r_{\text{core},c}(1 - r_{\text{core},c})/N)^{1/2}$$

where  $N$  denotes the total number of plaques sampled that contain color  $c$ .

Thus, the observed Cap+core frequencies are significantly higher for all four Confetti colors:

RFP	Cap	Core	Cap+core	N
Observed	6	9	48	63
Calculated ( $r \cdot N$ )	26	26	11	
error (SEM)	1.6	1.6	0.5	



YFP	Cap	Core	Cap+core	N
Observed	3	4	20	27
Calculated (r*N)	12	12	3	
Error (SEM)	1.1	1.1	0.2	

nGFP	Cap	Core	Cap+core	N
Observed	1	1	8	10
Calculated (r*N)	5	5	0.4	
Error (SEM)	0.8	0.8	0.02	

mCFP	Cap	Core	Cap+core	N
Observed	4	3	20	27
Calculated (r*N)	12	12	4	
Error (SEM)	1.1	1.1	0.2	

“Observed” is the measured number of cap only, core only and cap+core clones, “Calculated” is the expected number against the null hypothesis, and “Error” denotes the expected error (SEM) given the total number of clones that are measured (N).

### **Flow cytometry**

Single cell suspensions of VSMCs were obtained by enzymatic digestion of mouse aortas essentially as described previously<sup>4</sup>. Briefly, following removal of adipose and connective tissue, the samples were pre-digested in an enzyme mix (1 mg/ml Collagenase, Gibco, and 1 U/ml Elastase, Worthington, in Dulbecco’s Modified Eagles Medium) for 10 min at 37 °C after which the adventitia was peeled off and endothelial cells removed by gentle scraping. The medial layer was then incubated in fresh enzyme mix for 1-2 h with gentle agitation. Bone marrow was isolated from the femur and tibia and cells passed through a 40 µm cell strainer. Blood was collected by cardiac puncture following CO<sub>2</sub> asphyxiation and red blood cells lysed by incubation in 55 mM NH<sub>4</sub>Cl, 10 mM KHCO<sub>3</sub>, 0.1 mM EDTA (pH 7.3) for 10 min. Cell suspensions were then washed 3 times in PBS and analyzed on a BD Fortessa flow cytometer. Gates for fluorescent protein detection were defined based on VSMCs from wild type and labeled confetti animals.

### **Supplemental references**

1. Wirth A, Benyó Z, Lukasova M, Leutgeb B, Wettschureck N, Gorbey S, Örsy P, Horváth B, Maser-Gluth C, Greiner E, Lemmer B, Schütz G, Gutkind JS, Offermanns S. G12G13-LARG-mediated signaling in vascular smooth muscle is required for salt-induced hypertension. *Nature medicine*. 2008;14:64–68.
2. Snippert HJ, van der Flier LG, Sato T, van Es JH, van den Born M, Kroon-Veenboer C, Barker N, Klein AM, van Rheenen J, Simons BD, Clevers H. Intestinal crypt homeostasis results from neutral competition between symmetrically dividing Lgr5 stem cells. *CELL*. 2010;143:134–144.

- Piedrahita JA, Zhang SH, Hagaman JR, Oliver PM, Maeda N. Generation of mice carrying a mutant apolipoprotein E gene inactivated by gene targeting in embryonic stem cells. *Proceedings of the National Academy of Sciences*. 1992;89:4471–4475.
- Hamblin M, Chang L, Chen YE. *Isolation and Culture of Vascular smooth Muscle Cells*. Oxford, UK: John Wiley & Sons, Ltd; 2013:125–130.
- R Core Team (2016). R: A language and environment for statistical computing. R Foundation for Statistical Computing, Vienna, Austria. URL <https://www.R-project.org/>.

## Legends to Online Figures and Video

### Online Figure I: Frequency of Confetti reporter colors

Bar chart showing the proportions of each of the Confetti colors in VSMCs directly after recombination (light gray), in monochromatic regions within atherosclerotic plaques (dark gray) and in carotid ligation-induced neointimal patches (black). All data is from high density-labeled animals (10x 1 mg tamoxifen).

### Online Figure II: Mosaic labeling of medial VSMCs

**A**, Longitudinal cross section of a whole mount carotid artery from a Confetti animal labeled at high density (10x 1 mg tamoxifen). Signals for fluorescent proteins are shown with (i) and without (ii) nuclear DAPI (white). Arrows point to labeled VSMCs within the medial layer, arrow heads point to unlabeled cells within the endothelium and adventitia. The luminal side is denoted as "L" and the adventitial side marked "A". Scale bar is 50  $\mu$ m.

### Online Figure III: Specific labeling of VSMCs in Rosa26-Confetti+, Myh11-CreERT2+ animals

**A**, Flow cytometry analysis demonstrating background levels of fluorescence in bone marrow and peripheral blood from non-tamoxifen treated wild type animals and experimental Rosa26-Confetti+, Myh11-CreERT2+ animals labeled at high density (10x 1 mg tamoxifen). Samples were gated for live cells (FSC-A, SSC-A) and singlets (FSC-A, FSC-H). Negative cells were identified based on gates set on VSMCs from wild type and Confetti animals. **B**, Confocal microscopy images showing absence of recombination in liver (i, iv), skeletal muscle (ii, v) and lung (iii, vi) in Confetti animals after tamoxifen treatment (10x 1 mg). Note, that labeled cells in (vi) correspond to VSMCs lining a blood vessel. Signals for fluorescent proteins are shown with (i, ii, iii) and without nuclear DAPI staining (white, iv, v, vi). Scale bars are 100  $\mu$ m.

### Online Figure IV: Histological analysis of monochromatic plaque region

**A**, Haematoxylin and eosin staining of 20  $\mu$ m cryosections from HFD treated Confetti animal labeled at high density (10x 1 mg tamoxifen). For comparison, the signals from fluorescent proteins in an adjacent section are shown with (B) and without nuclear DAPI staining (white, C). Scale bars are 100  $\mu$ m.

### Online Figure V: Proportion of plaque cells expressing the Confetti reporter

**A**, Box plot quantifying the proportion of all cells (DAPI) within plaques from different regions of the vasculature which express the Confetti reporter (Confetti+). **B**, **C**, Box plots showing the proportion of cells expressing the Confetti reporter (Confetti+), which were stained for either aSma or Mac3 (Confetti+ Stain+) within plaques from different regions of the vasculature (B) or different animals (C). Red stars indicate a significant difference based on a two-way ANOVA,  $p < 0.05$ , data from 23 plaques from 6 animals labeled at high density (10x 1 mg tamoxifen). Arch: aortic arch, DA: descending aorta, CA: carotid artery.

### **Online Figure VI: Clonal VSMC expansion in atherosclerotic plaques**

Examples of monochromatic plaques (**A**) and plaques containing VSMC-derived cells of more than one color (**B-D**). **B**, example of a plaque containing two intermingled clones (yellow and green). The section shown in panel (**D**) is cut through the top of the aortic arch and includes a portion of the right carotid artery. Signals from fluorescent proteins in 50-100  $\mu\text{m}$  vibratome sections are shown with (i) and without nuclear DAPI staining (white, ii). All plaques are from animals labeled at high density (10x 1 mg tamoxifen). Scale bars are 100 (**A-C**) and 200  $\mu\text{m}$  (**D**). A video of the plaque shown in panel **A** is provided as Supplemental Online Video I.

### **Online Figure VII: Animals labeled at medium density develop plaques with large monochromatic regions, which span both the cap and core**

**A**, An atherosclerotic plaque from a medium density-labeled (1x 1 mg tamoxifen) Confetti animal following 16 weeks of high fat diet. Signals from fluorescent proteins are shown with (i) and without (ii) nuclear DAPI (white). Scale bars are 100  $\mu\text{m}$ .

### **Online Figure VIII: Proportion of all cells within atherosclerotic plaques and injury-induced neointima which are VSMC-derived cells and express phenotype marker proteins**

**A-C**, Box plots displaying the proportion of all plaque cells (DAPI) co-expressing the Confetti reporter and either aSma or Mac3 (Confetti+ Stain+) according to plaque region (**A**), individual animals (**B**) and vascular region (**C**) in high density-labeled (10x 1 mg tamoxifen) Rosa26-Confetti+, Myh11-CreERT2+, ApoE<sup>-/-</sup> animals after high fat diet. **D**, Proportion of total number of cells (DAPI) which co-express the Confetti reporter and either aSma or Mac3 (Confetti+ Stain+) in carotid ligation-induced neointima from high density-labeled (10x 1 mg tamoxifen) Rosa26-Confetti+, Myh11-CreERT2+ animals 28 days post-surgery.

### **Online Figure IX: Number and distribution of Confetti colors within atherosclerotic plaques**

**A-E**, Bar charts showing the proportion of plaques in high density (10x 1 mg tamoxifen, **A**, **C-E**) and medium density (1x 1 mg tamoxifen, **B**) labeled animals with one, two, three or four colors. Bars represent the entire plaque (dark gray), the cap (light gray) or the core of the plaque (black). **C**, **D**, **E**, Data is shown for plaques in different vascular regions (**C**, Aortic Arch; **D**, Descending aorta; **E**, Carotid artery). **F**, Bar chart showing the proportion of monochromatic regions within plaques which occupy the plaque cap only (dark gray), core only (light gray) or both the core and cap (black). Data is shown for high density (10x 1 mg), low density-labeled (1x 1 mg) or all animals at the left, and stratified according to vascular regions on the right. Arch: aortic arch, DA: descending aorta, CA: carotid artery.

### **Online Figure X: Right carotid artery immunostaining controls**

**A-D**, Single confocal scans from Z-stacks of 14  $\mu\text{m}$  cryosections from the control right carotid artery of high density-labeled (10x 1 mg tamoxifen) animal 28 days after ligation of the left carotid artery stained for aSma (**A**), Mac-3 (**B**), Smmhc/Myh11 (**C**) or EdU (**D**). For each staining, (ii-iv) are zoomed images of the regions outlined in (i). Signals for fluorescent proteins, DAPI (white), aSma (magenta), Mac3 (magenta), EdU (magenta), and Smmhc (magenta) are shown as indicated on each image. Scale bars are 50  $\mu\text{m}$ .

### **Online Figure XI: Smmhc and EdU staining in carotid ligation-induced neointima**

**A**, **B**, Single confocal scans from Z-stacks of 14  $\mu\text{m}$  cryosections from the left carotid artery 28 days post-ligation in a high density-labeled animal (10x 1 mg tamoxifen) stained for Smmhc (**A**) or EdU (**B**). For each staining, the region outlined in (i) is magnified in (ii-iv). Arrows point to cells co-expressing the Confetti reporter and Smmhc (**A**) or EdU (**B**), whereas arrow heads point to cells that express the Confetti reporter, but do not stain for the

respective marker. Signals for fluorescent proteins, DAPI (white), Smmhc (magenta) and EdU (magenta) are shown as indicated on each image. Scale bars are 50  $\mu\text{m}$ .

**Online Figure XII: Clonal patches span both media and neointima**

Longitudinal cross section of the left carotid artery from animals labeled at high density (10x 1 mg tamoxifen, **i**) or low density (1x 0.1 mg tamoxifen, **ii**), which were analyzed 28 days post-surgery, showing that individual VSMC-derived clones are “anchored” in the medial layer. A single scan of a confocal Z-stack, which intersects the middle of the vessel, is shown. Signals for fluorescent proteins and DAPI (white) are shown. Scale bars are 100  $\mu\text{m}$ .

**Online Figure XIII: Proliferative VSMC-derived cells detected within both the core and cap of atherosclerotic plaques**

**A, B**, Cryosections of atherosclerotic plaques from Confetti animals subjected to 16 weeks of high fat diet and injected with EdU 2 hours before analysis. The regions outlined in (**i**) are magnified in (**ii-iv**). Arrows point to EdU-positive cells expressing the Confetti reporter in the cap (**A**) or core region (**B**). Signals for fluorescent proteins, DAPI (white) and EdU (magenta) are shown as indicated on each image. **C, D**, Box plot showing the proportion of cells expressing the Confetti reporter (Confetti+) which are EdU+ (Confetti+ EdU+) displayed for all areas analyzed (**C**) and separately for the plaque cap, core and shoulder regions (**D**). **E**, Box plot showing the proportion of all cells (DAPI) which are EdU+. Data in (**C-E**) is from 9 plaques from 5 animals. All data is from high density-labeled animals.

**Online Video I: Clonal VSMC expansion in atherosclerotic plaques**

This video shows a 100  $\mu\text{m}$  thick vibratome section from a carotid artery containing an atherosclerotic plaque formed of VSMCs of one color. Initially only GFP signal is shown, then YFP, CFP and RFP signals are added and finally the signal from nuclear DAPI staining (white). During the video DAPI is removed and shown again while the video demonstrates that VSMCs of a single color can occupy core and cap regions in a thick slice from an atherosclerotic plaque. The plaque shown in the video is also shown (Z-stack projection) in Online Figure VI, A. The scale bar and displayed size adjusts automatically as the video is played.

**Online Table I. Efficiency of VSMC labeling in high density (10x 1 mg tamoxifen) and low density-labeled animals (1x 0.1 mg tamoxifen)**

Cell I.D., Tamoxifen dose	Fluorescently labeled (%)			Non-labeled (%)		
	Average	Max	Min	Average	Max	Min
VSMC wild type, 10 mg (n=1)	0	NA	NA	100	NA	NA
VSMC Confetti, 10 mg (n=6)	78.5	92.9	69.6	21.5	30.4	7.1
VSMC Confetti, 0.1 mg (n=3)	0.8	1.0	0.5	99.2	99.5	99.0

\*NA: Not applicable

**Online Table II: Experimental animals used for atherosclerosis studies**

Animal no.	Back-crosses*	Tamoxifen dose (mg)	HFD (weeks)	Plaques analyzed	Analysis method
1	2	10	17	4	vibratome
2	2	10	12 <sup>†</sup>	2	vibratome
3	2	10	19	10	vibratome
4	2	10	18	8	cryo
5	2	10	18	8	cryo
6	2	10	18	7	cryo
7	2	10	14 <sup>†</sup>	9	cryo
8	2	10	18	8	cryo
9	2	10	17	10	cryo
10	2	10	17	1	vibratome
11	2	10	16	2	cryo
12	2	10	16	2	cryo
13	2	10	16	4	cryo
14	2	10	16	3	cryo
15	2	10	16	3	cryo
16	2	10	16	1	cryo
17	2	1	16	2	cryo
18	2	1	16	3	cryo
19	2	1	16	4	cryo
20	2	1	16	4	cryo
21	2	1	16	1	cryo
22	2	0.1	13 <sup>†</sup>	0 <sup>‡</sup>	vibratome
23	2	0.1	11 <sup>†</sup>	0	vibratome
24	2	0.1	14	0	vibratome
25	2	0.1	14	0	vibratome

\* Number of backcrosses to C57Bl/6.

† Animals were analyzed prematurely due to health issues unrelated to cardiovascular defects (e.g. fighting or warts).

‡ One monochromatic region was observed, but this was not included in any analysis.

**Online Table III: Plaque information**

Animal no.	Plaque no.	Tamoxifen dose (mg)	Vascular Region*	Colors per plaque	aSma	Mac3	DS <sup>†</sup>	EdU
1	1 <sup>‡</sup>	10	CA	2 (RFP, YFP)	-	-	-	-
1	2	10	DA	2 (RFP, YFP)	-	-	-	-
1	3	10	AA	1 (RFP)	-	-	-	-
1	4	10	CA	2 (YFP, nGFP)	-	-	-	-
2	5	10	AA	2 (RFP, mCFP)	-	-	-	-
2	6	10	AA	2 (nGFP, RFP)	-	-	-	-
3	7	10	CA	2 (nGFP, RFP)	-	-	-	-
3	8 <sup>‡</sup>	10	CA	2 (YFP, nGFP)	-	-	-	-
3	9 <sup>‡</sup>	10	AA	2 (RFP, mCFP)	-	-	-	-
3	10	10	AA	2 (RFP, YFP)	-	-	-	-
3	11 <sup>‡</sup>	10	AA	2 (RFP, mCFP)	-	-	-	-
3	12	10	CA	1 (RFP)	-	-	-	-
3	13	10	CA	1 (RFP)	-	-	-	-
3	14	10	CA	2 (RFP, YFP)	-	-	-	-
3	15	10	CA	1 (YFP)	-	-	-	-
3	16	10	AA	2 (RFP, nGFP)	-	-	-	-
4	17	10	CA	1 (YFP)	-	-	-	-
4	18	10	CA	2 (mCFP, nGFP)	+	+	-	-
4	19	10	AA	2 (RFP, mCFP)	-	-	-	-
4	20	10	AA	2 (RFP, YFP)	-	-	-	-
4	21	10	AA	1 (RFP)	+	+	+	-
4	22	10	AA	1 (YFP)	-	-	-	-
4	23 <sup>‡</sup>	10	DA	1 (RFP)	+	+	+	-
4	24	10	?	1 (RFP)	-	-	-	-
5	25 <sup>‡</sup>	10	DA	3 (RFP, YFP, mCFP)	+	+	-	-
5	26 <sup>‡</sup>	10	CA	1 (RFP)	+	+	-	-
5	27	10	AA	2 (RFP, mCFP)	-	-	-	-
5	28 <sup>‡</sup>	10	CA	1 (RFP)	+	+	-	-
5	29	10	AA	1 (mCFP)	+	+	-	-
5	30	10	AA	1 (RFP)	+	+	-	-
5	31	10	?	1 (RFP)	-	-	-	-
5	32	10	?	1 (RFP)	-	-	+	-
6	33	10	CA	1 (RFP)	-	-	-	-
6	34	10	CA	1 (mCFP)	-	-	-	-
6	35	10	CA	1 (mCFP)	+	+	-	-
6	36	10	AA	1 (RFP)	-	-	+	-
6	37	10	DA	1 (RFP) <sup>§</sup>	+	+	-	-
6	38	10	AA	1 (mCFP)	+	+	-	-
6	39	10	DA	1 (RFP)	+	+	-	-
7	40	10	DA	1 (mCFP)	-	-	-	-
7	41 <sup>‡</sup>	10	DA	1 (mCFP)	-	-	-	-
7	42	10	DA	1 (RFP)	-	-	+	-
7	43	10	CA	2 (RFP, YFP)	+	+	-	-
7	44	10	AA	2 (RFP, YFP)	+	+	-	-
7	45	10	?	4 (RFP, YFP, mCFP, nGFP)	+	+	-	-
7	46	10	CA	1 (YFP)	-	-	-	-
7	47	10	AA	2 (RFP, mCFP)	+	+	+	-
7	48	10	?	2 (RFP, nGFP)	-	-	-	-
8	49	10	DA	1 (RFP)	-	-	-	-
8	50	10	DA	1 (mCFP)	+	+	-	-
8	51	10	?	1 (RFP)	-	-	-	-
8	52	10	AA	2 (RFP, mCFP)	-	-	-	-
8	53	10	AA	1 (RFP)	+	+	+	-
8	54	10	DA	2 (RFP, mCFP)	+	+	-	-
8	55	10	CA	2 (RFP, YFP)	+	+	-	-
8	56	10	AA	2 (mCFP, RFP)	-	-	-	-
9	57	10	AA	3 (RFP, YFP, mCFP)	-	-	-	-
9	58	10	AA	1 (RFP)	-	-	-	-
9	59	10	DA	1 (RFP)	-	-	-	-
9	60	10	AA	2 (mCFP, RFP)	+	+	+	-
9	61	10	AA	1 (YFP)	-	-	-	-
9	62	10	AA	1 (RFP)	-	-	-	-

9	63	10	AA	2 (RFP, YFP)	+	+	-	-
9	64	10	DA	1 (RFP)	-	-	-	-
9	65	10	?	3 (mCFP, RFP, YFP)	-	-	-	-
9	66	10	DA	1 (mCFP)	-	-	-	-
10	67	10	DA	1 (YFP)	-	-	-	-
11	68	10	CA	3 (RFP, YFP, mCFP)	-	-	-	-
11	69	10	CA	1 (RFP)	-	-	-	+
12	70	10	AA	2 (RFP, YFP)	-	-	-	+
12	71	10	DA	1 (YFP)	-	-	-	-
13	72	10	CA	2 (RFP, nGFP)	-	-	-	+
13	73 <sup>‡</sup>	10	DA	2 (RFP, mCFP)	-	-	-	+
13	74	10	AA	1 (RFP)	-	-	-	+
13	75	10	DA	2 (YFP, nGFP)	-	-	-	+
14	76	10	AA	1 (RFP)	-	-	-	+
14	77	10	CA	2 (RFP, YFP)	-	-	-	-
14	78	10	CA	3 (mCFP, RFP, YFP)	-	-	-	+
15	79	10	AA	1 (RFP)	-	-	-	-
15	80 <sup>‡</sup>	10	CA	2 (RFP, mCFP)	-	-	-	+
15	81	10	CA	1 (RFP)	-	-	-	-
16	82	10	CA	1 (YFP)	-	-	-	-
17	83	1	AA	1 (RFP)	-	-	-	-
17	84	1	AA	2 (RFP, YFP)	-	-	-	-
18	85	1	AA	1 (RFP)	-	-	-	-
18	86	1	CA	1 (RFP)	-	-	-	-
18	87	1	DA	1 (YFP)	-	-	-	-
19	88	1	AA	1 (RFP)	-	-	-	-
19	89	1	AA	2 (RFP, YFP)	-	-	-	-
19	90	1	CA	1 (RFP)	-	-	-	-
19	91	1	CA	1 (RFP)	-	-	-	-
20	92 <sup>‡</sup>	1	DA	1 (RFP)	-	-	-	-
20	93 <sup>‡</sup>	1	DA	2 (RFP, YFP)	-	-	-	-
20	94	1	CA	1 (RFP)	-	-	-	-
20	95	1	AA	1 (RFP)	-	-	-	-
21	96	1	AA	1 (RFP)	-	-	-	-

\* AA: ascending aorta or aortic arch. DA: descending aorta. CA: carotid artery or brachiocephalic artery. Plaques at borders between vascular regions are indicated with a question mark.

† DS: double staining for aSma and Mac3. Only done in plaques that did not contain nGFP or YFP positive cells.

‡ Displayed in figure (Plaque #1: Online Figure VI, C; #8: Online Figure VI, B; #9: Online Figure VI, D; ; #11: Online Figure VI, A, Online Video I; ; #23: Figure 4B; ; #25: Figure 2C; #26: Figure 3AB, Online Figure IV; ; #28: Figure 5AB; ; #41: Figure 2B; ; #73: Online Figure XIII A; ; #80: Online Figure XIII, B; #92,93: Online Figure VII).

§ One YFP-expressing cell was observed in this plaque.



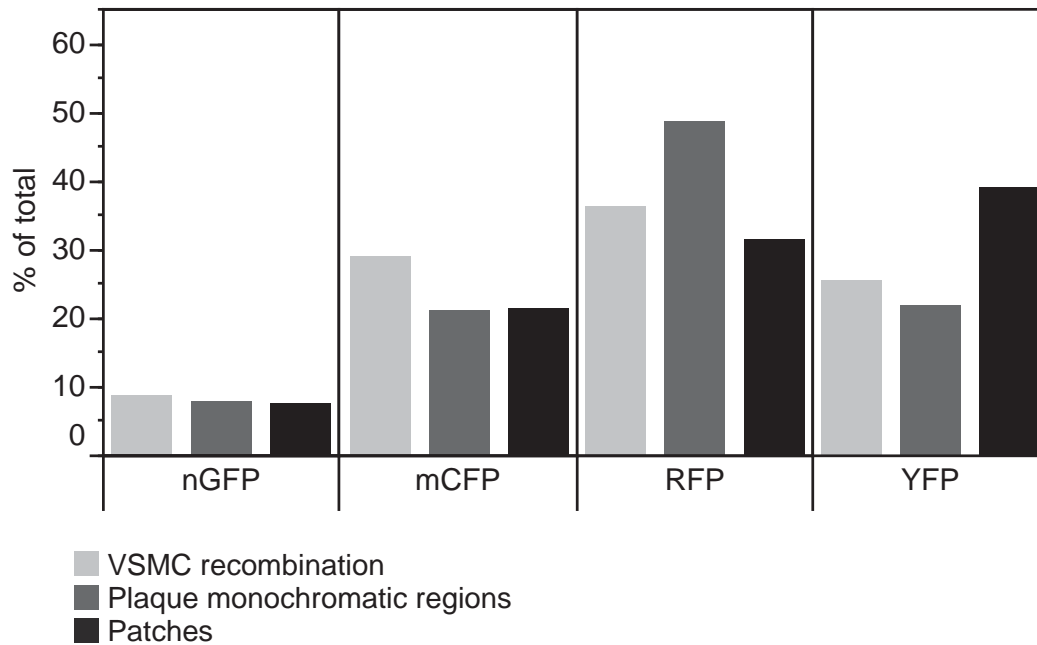
**Online Table IV: Experimental animals used for carotid ligation surgery**

Animal no.	Tamoxifen dose (mg)	Back-crosses*	nGFP	YFP	RFP	mCFP	Confetti patches	Measured patches†	Patch size (cell number)	Remodeled area (μm)
1	10	1	3	6	7	4	20	17	48, 52, 149, 156, 227, 375, 425, 522, 585, 872, 950, 981, 1040, 1990, 2290, 3140, 3450	4517
2‡	10	1	1	2	1	3	7	7	171, 409, 666, 849, 940, 1470, 3610	2391
3	10	1	1	1	0	1	3	1	178	1301
4	10	1	0	2	2	0	4	4	174, 332, 415, 508	1878
5	10	1	0	1	1	1	3	3	66, 360, 3090	1276
6	10	1	0	1	2	0	3	3	125, 151, 329	1130
7	10	1	0	2	1	1	4	3	128, 234, 7480	1609
8	10	1	0	3	3	1	7	3	52, 149, 446	2128
9	10	1	0	2	2	2	6	3	125, 805, 1495	1345
10	10	1	0	2	1	1	4	3	96, 115, 1490	1503
11‡	10	6	0	1	1	1	3	3	565, 612, 3200	1994
12	10	6	0	1	1	1	3	2	1097, 2827	2816
13	1	6	0	3	1	2	6	4	35, 63, 689, 1073	NA
14	1	5	2	2	2	0	6	6	50, 55, 81, 98, 148, 225	NA
15	1	6	0	1	1	0	2	2	9, 64	NA
16	1	6	0	1	1	1	3	3	24, 153, 410	NA
17	0.1	1	0	0	0	0	0	0	NA	NA
18	0.1	1	0	1	0	1	2	2	45, 170	NA
19	0.1	1	0	0	0	0	0	0	NA	NA
20‡	0.1	1	0	2	1	0	3	3	65, 192, 749	NA
21	0.1	1	0	0	0	0	0	0	NA	NA
22	0.1	5	0	1	0	0	1	1	32	NA
23	0.1	6	0	1	1	0	2	2	59, 592	NA

\* Number of backcrosses to C57Bl/6.

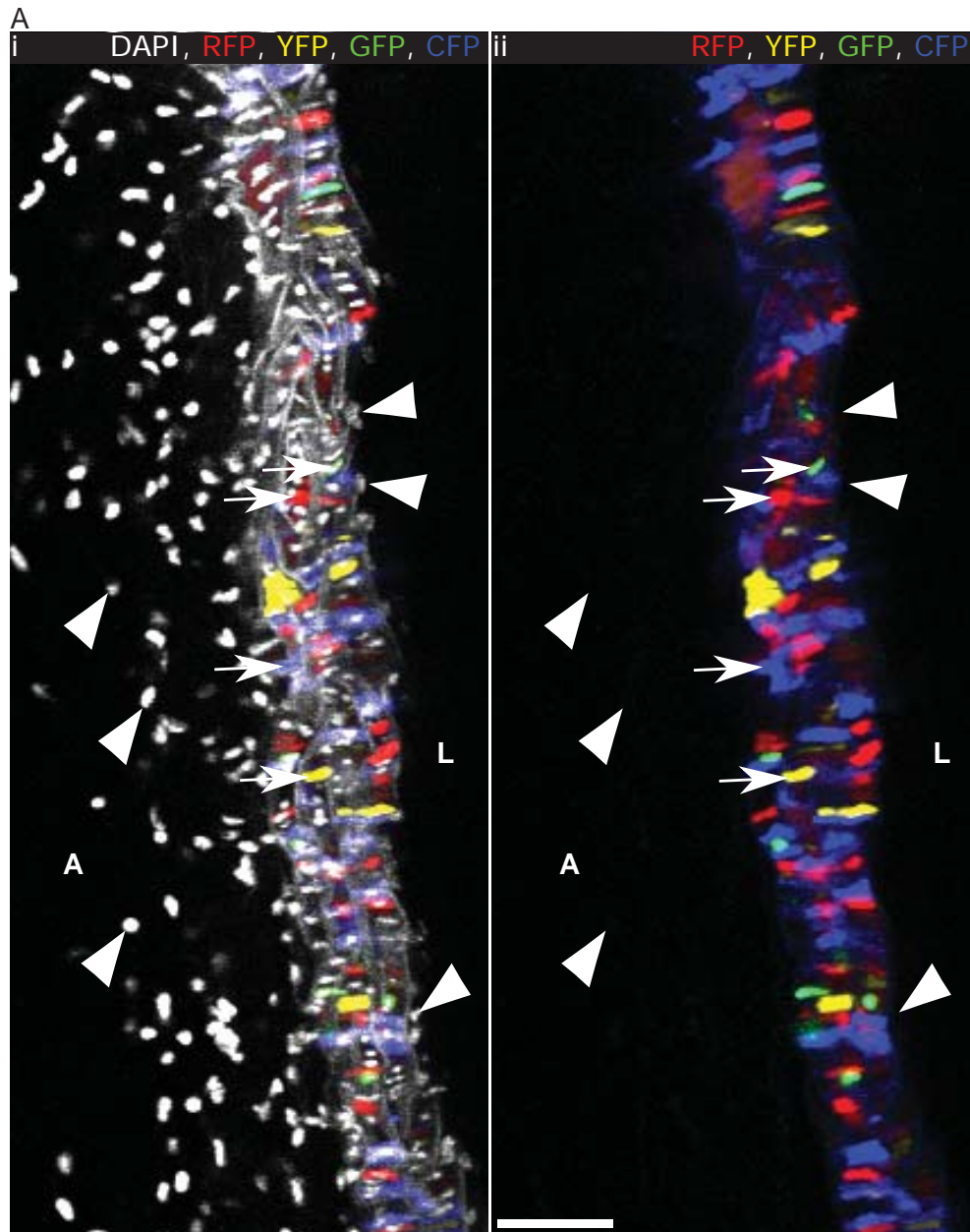
† A small subset of patches was not quantified due to technical issues, such as high autofluorescence, which impeded surface modeling in Imaris.

‡ Displayed in figure (Animal #2: Figure 6BC, Online Figure XII, i; #11: Figure 7AB, Online Figure X, Online Figure XI; #20: Figure 6E, Online Figure XII, ii).  
NA, not applicable.



**Online Figure I: Frequency of Confetti reporter colors**

Bar chart showing the proportions of each of the Confetti colors in VSMCs directly after recombination (light gray), in monochromatic regions within atherosclerotic plaques (dark gray) and in carotid ligation-induced neointimal patches (black). All data is from high density-labeled animals (10x 1 mg tamoxifen)



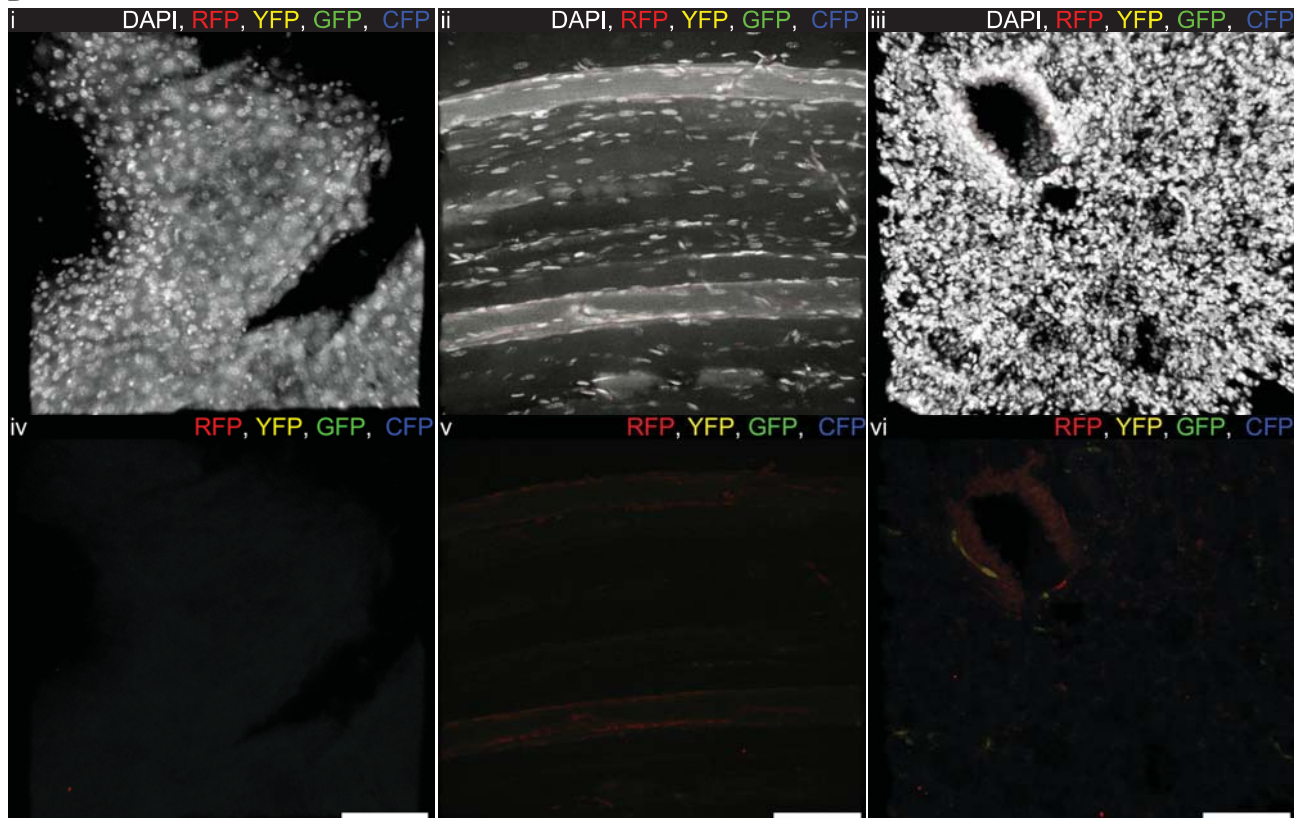
**Online Figure II: Mosaic labeling of medial VSMCs**

**A**, Longitudinal cross section of a whole mount carotid artery from a Confetti animal labeled at high density (10x 1 mg tamoxifen). Signals for fluorescent proteins are shown with (i) and without (ii) nuclear DAPI (white). Arrows point to labeled VSMCs within the medial layer, arrow heads point to unlabeled cells within the endothelium and adventitia. The luminal side is denoted as "L" and the adventitial side marked "A". Scale bar is 50  $\mu$ m.

A

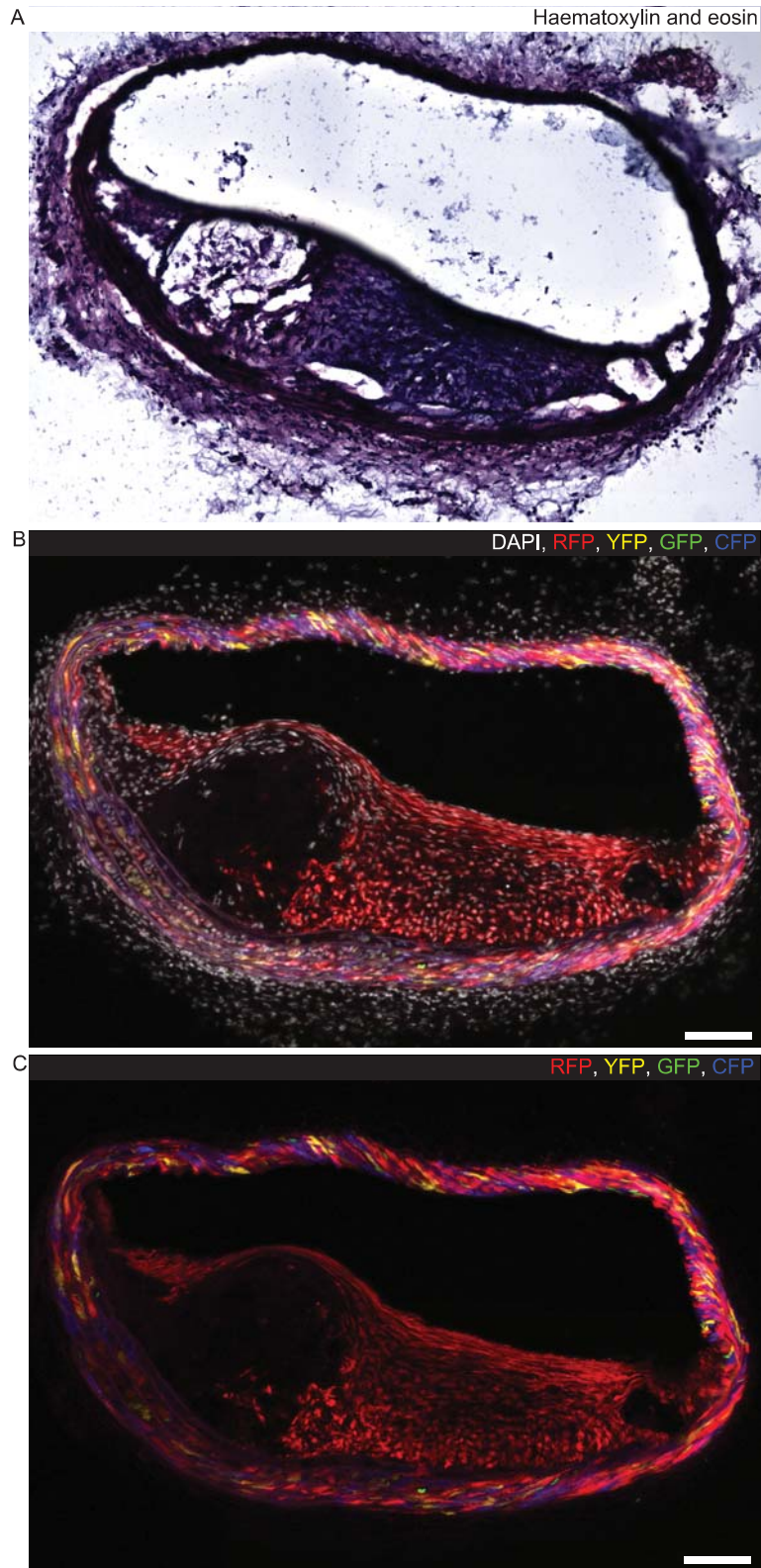
Mouse no.	ID	Sample	Proportion of positive events	Number of singlet events
1	Wild type	Peripheral blood	0.0006	>25000
2	Wild type		0.0003	>65000
3	Wild type		0.00007	>65000
4	Confetti+		0.0001	>65000
5	Confetti+		0.00009	>65000
6	Confetti+		0.0001	>65000
1	Wild type	Bone marrow	0.00002	>400000
2	Wild type		0.00001	>400000
3	Wild type		0.00007	>200000
4	Confetti+		0.00001	>400000
5	Confetti+		0	>400000
6	Confetti+		0.00002	>400000
1	Wild type	Aorta	0.0002	>9000
2	Wild type		0.0001	>30000
3	Wild type		0.0005	>30000
4	Confetti+		0.62	>30000
5	Confetti+		0.63	>30000
6	Confetti+		0.67	>30000

B



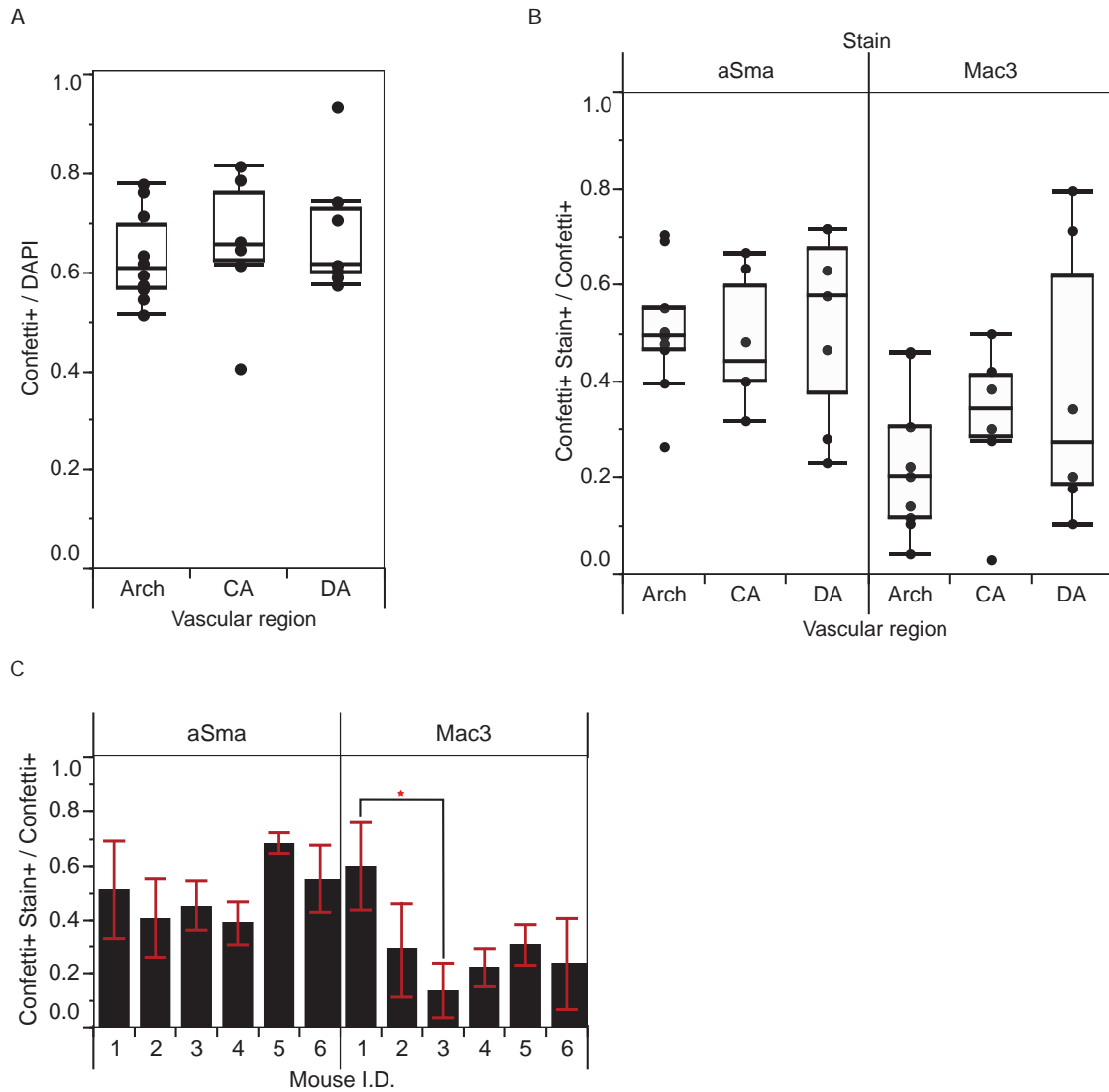
### Online Figure III: Specific labeling of VSMCs in Rosa26-Confetti+, Myh11-CreERT2+ animals

**A**, Flow cytometry analysis demonstrating background levels of fluorescence in bone marrow and peripheral blood from non-tamoxifen treated wild type animals and experimental Rosa26-Confetti+, Myh11-CreERT2+ animals labeled at high density (10x 1 mg tamoxifen). Samples were gated for live cells (FSC-A, SSC-A) and singlets (FSC-A, FSC-H). Negative cells were identified based on gates set on VSMCs from wild type and Confetti animals. **B**, Confocal microscopy images showing absence of recombination in liver (**i**, **iv**), skeletal muscle (**ii**, **v**) and lung (**iii**, **vi**) in Confetti animals after tamoxifen treatment (10x 1 mg). Note, that labeled cells in (**vi**) correspond to VSMCs lining a blood vessel. Signals for fluorescent proteins are shown with (**i**, **ii**, **iii**) and without nuclear DAPI staining (white, **iv**, **v**, **vi**). Scale bars are 100 μm.



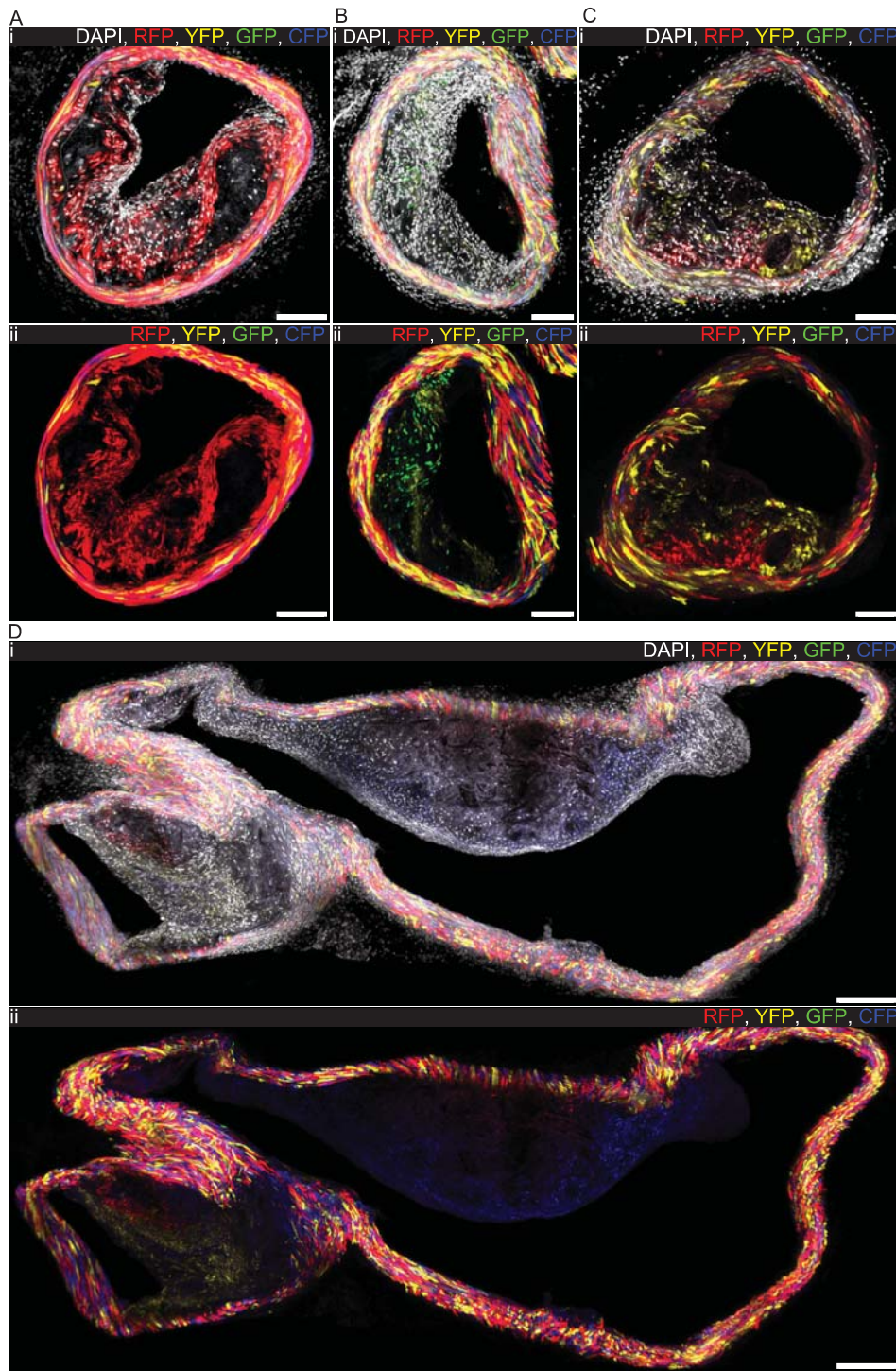
**Online Figure IV: Histological analysis of monochromatic plaque region**

**A**, Haematoxylin and eosin staining of 20  $\mu\text{m}$  cryosections from HFD treated Confetti animal labeled at high density (10x 1 mg tamoxifen). For comparison, the signals from fluorescent proteins in an adjacent section are shown with **(B)** and without nuclear DAPI staining (white, **C**). Scale bars are 100  $\mu\text{m}$ .



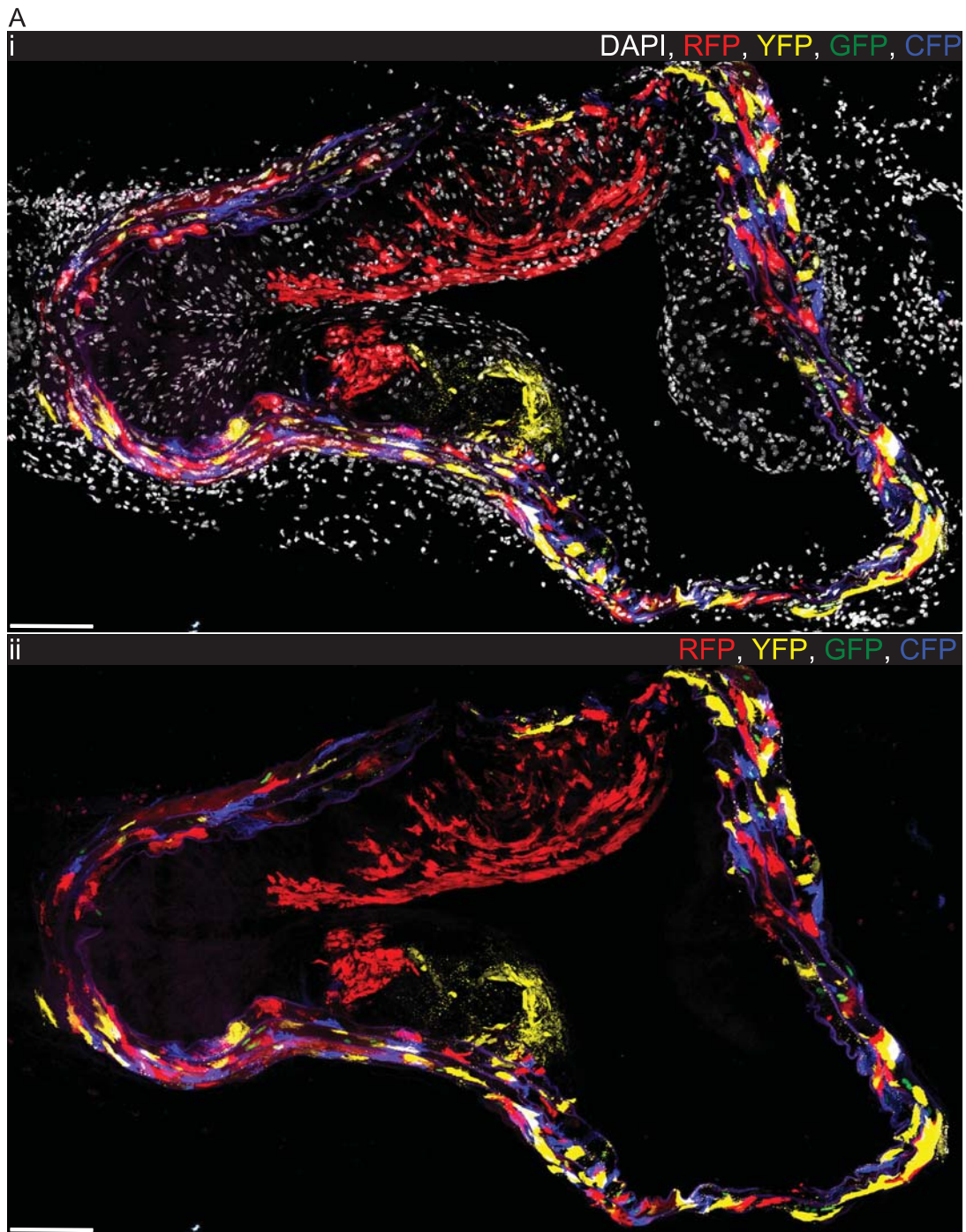
**Online Figure V: Proportion of plaque cells expressing the Confetti reporter**

**A**, Box plot quantifying the proportion of all cells (DAPI) within plaques from different regions of the vasculature which express the Confetti reporter (Confetti+). **B**, **C**, Box plots showing the proportion of cells expressing the Confetti reporter (Confetti+), which were stained for either aSma or Mac3 (Confetti+ Stain+) within plaques from different regions of the vasculature (**B**) or different animals (**C**). Red stars indicate a significant difference based on a two-way ANOVA,  $p < 0.05$ , data from 23 plaques from 6 animals labeled at high density (10x 1 mg tamoxifen). Arch: aortic arch, DA: descending aorta, CA: carotid artery.



**Online Figure VI: Clonal VSMC expansion in atherosclerotic plaques**

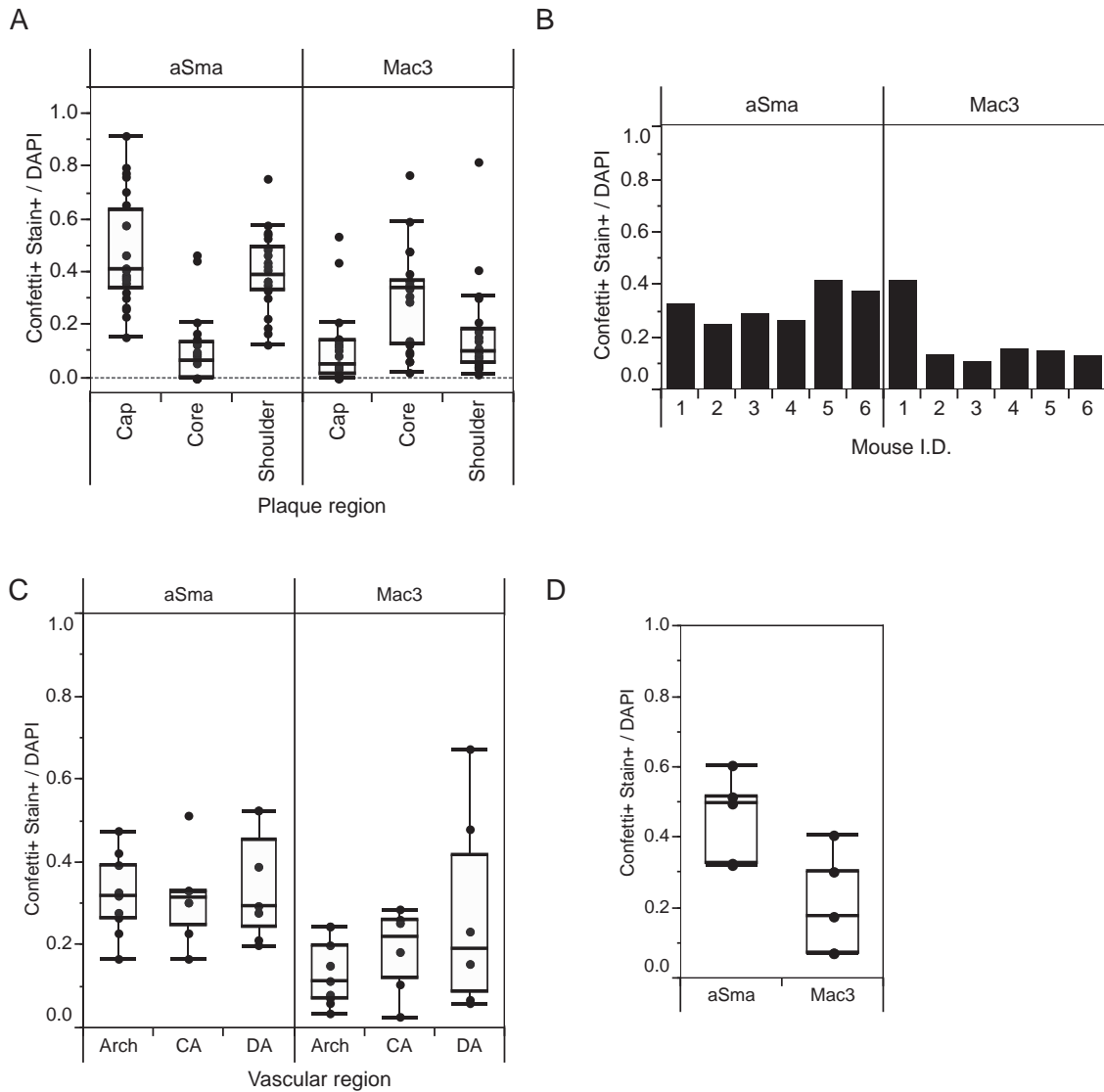
Examples of monochromatic plaques (**A**) and plaques containing VSMC-derived cells of more than one color (**B-D**). **B**, example of a plaque containing two intermingled clones (yellow and green). The section shown in panel (**D**) is cut through the top of the aortic arch and includes a portion of the right carotid artery. Signals from fluorescent proteins in 50-100  $\mu\text{m}$  vibratome sections are shown with (i) and without nuclear DAPI staining (white, ii). All plaques are from animals labeled at high density (10x 1 mg tamoxifen). Scale bars are 100 (**A-C**) and 200  $\mu\text{m}$  (**D**). A video of the plaque shown in panel **A** is provided as Supplemental Online Video I.



**Online Figure VII: Animals labeled at medium density develop plaques with large monochromatic regions, which span both the cap and core**

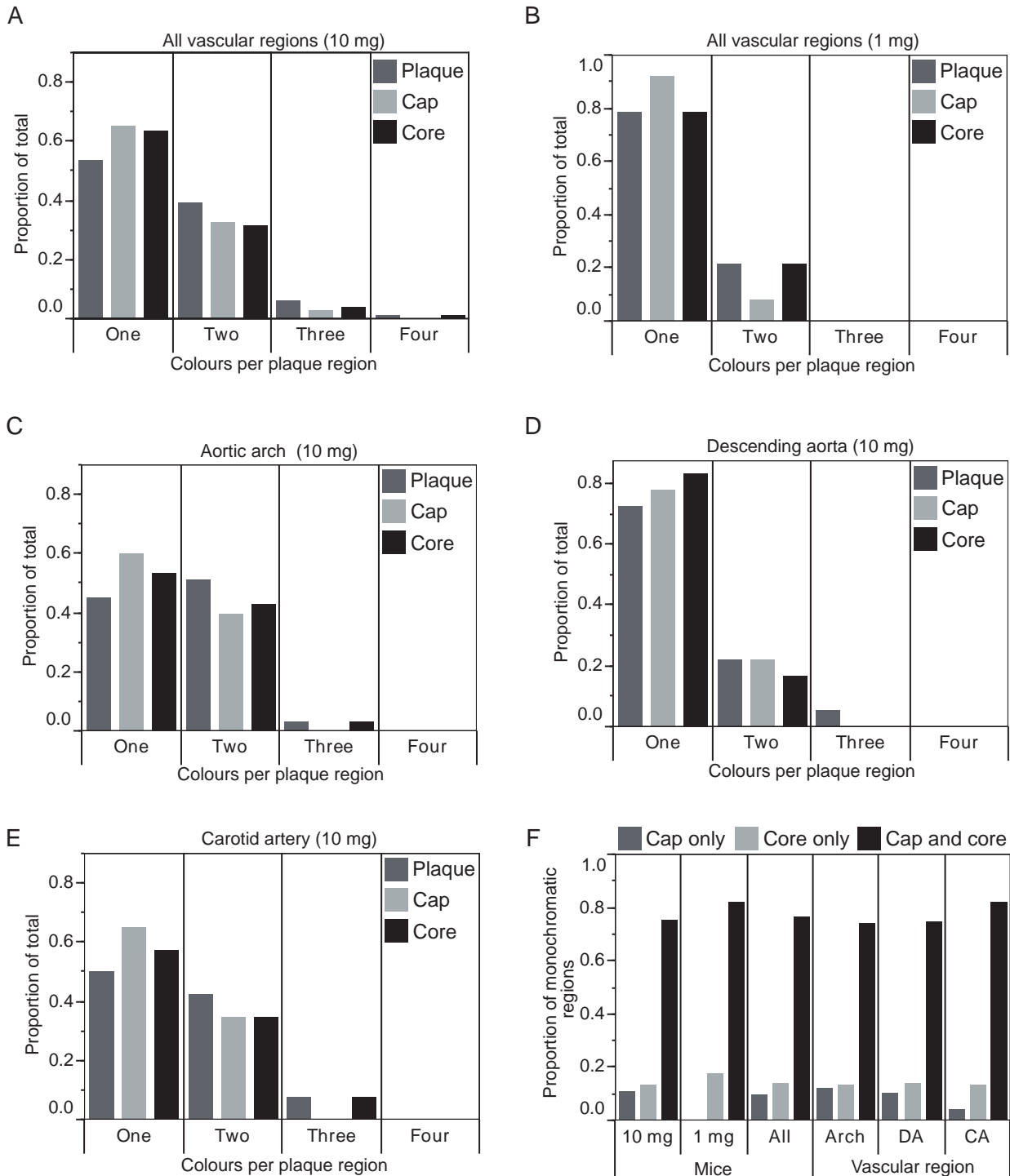
**A**, An atherosclerotic plaque from a medium density-labeled (1x 1 mg tamoxifen) Confetti animal following 16 weeks of high fat diet. Signals from fluorescent proteins are shown with (i) and without (ii) nuclear DAPI (white). Scale bars are 100  $\mu$ m.





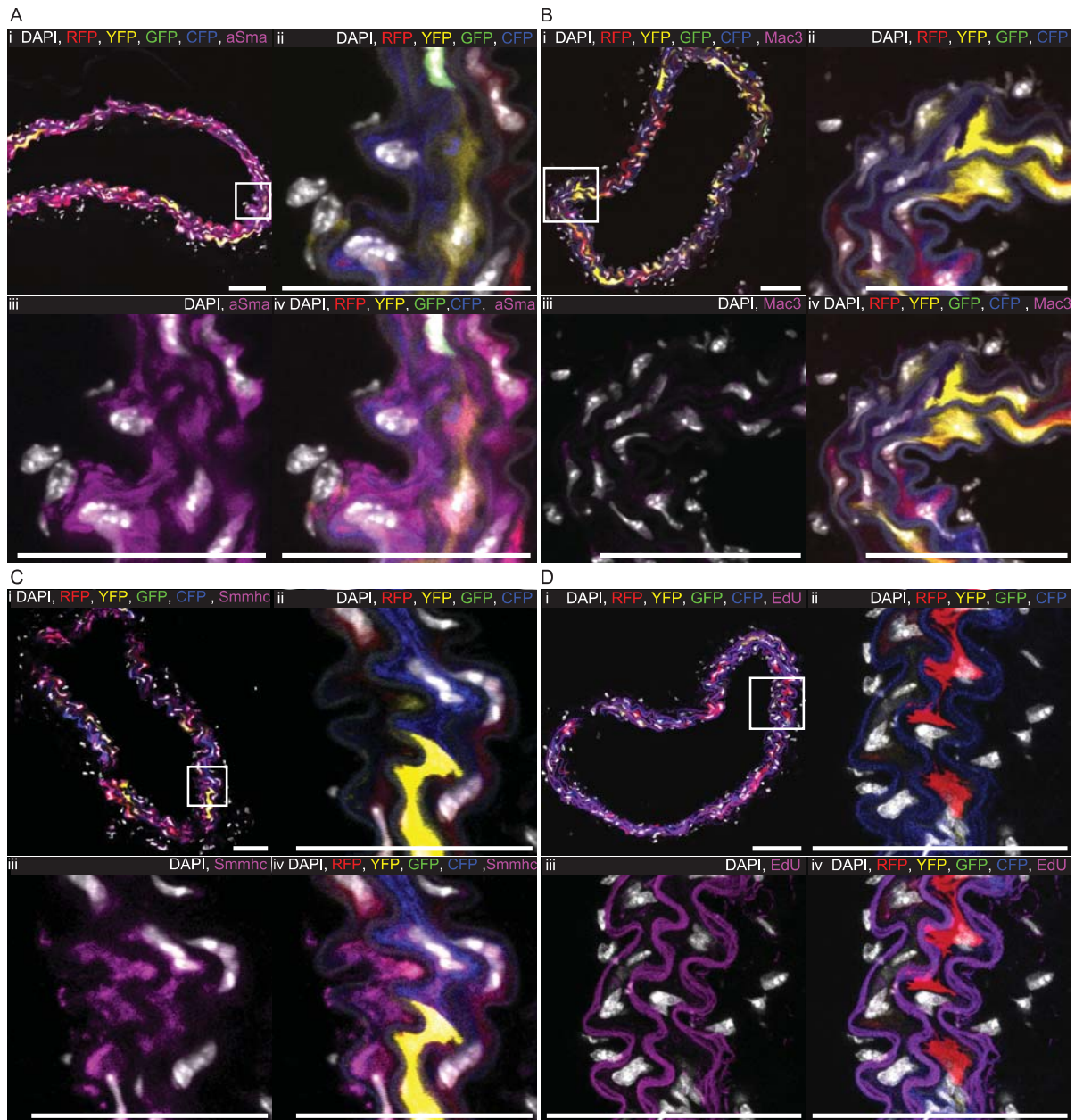
**Online Figure VIII: Proportion of all cells within atherosclerotic plaques and injury-induced neointima which are VSMC-derived cells and express phenotype marker proteins**

**A-C**, Box plots displaying the proportion of all plaque cells (DAPI) co-expressing the Confetti reporter and either aSma or Mac3 (Confetti+ Stain+) according to plaque region (**A**), individual animals (**B**) and vascular region (**C**) in high density-labeled (10x 1 mg tamoxifen) Rosa26-Confetti+, Myh11-CreERT2+, ApoE<sup>-/-</sup> animals after high fat diet. **D**, Proportion of total number of cells (DAPI) which co-express the Confetti reporter and either aSma or Mac3 (Confetti+ Stain+) in carotid ligation-induced neointima from high density-labeled (10x 1 mg tamoxifen) Rosa26-Confetti+, Myh11-CreERT2+ animals 28 days post-surgery



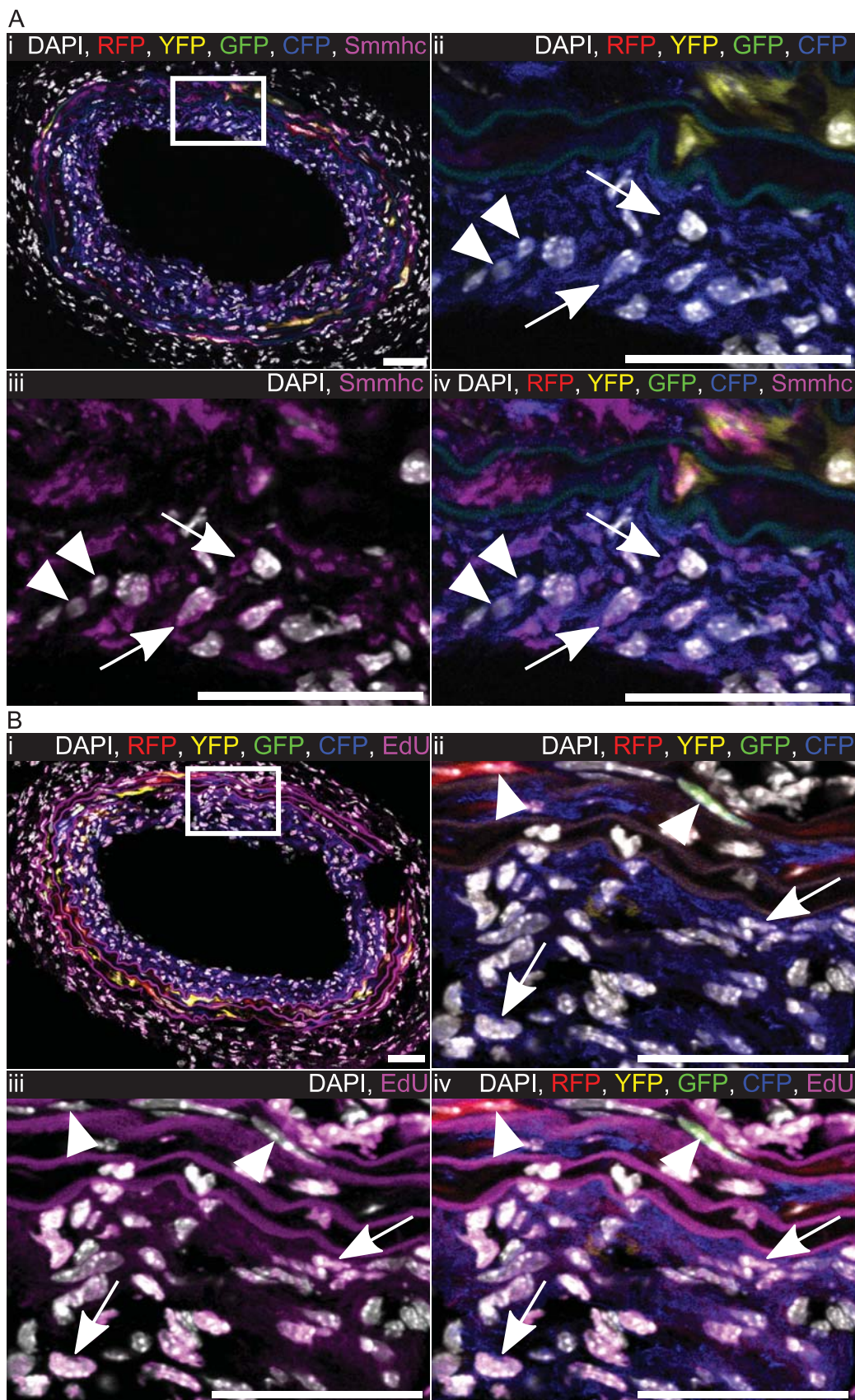
### Online Figure IX: Number and distribution of Confetti colors within atherosclerotic plaques

**A-E**, Bar charts showing the proportion of plaques in high density (10x 1 mg tamoxifen, **A**, **C**, **E**) and medium density (1x 1 mg tamoxifen, **B**) labeled animals with one, two, three or four colors. Bars represent the entire plaque (dark gray), the cap (light gray) or the core of the plaque (black). **C**, **D**, **E**, Data is shown for plaques in different vascular regions (**C**, Aortic Arch; **D**, Descending aorta; **E**, Carotid artery). **F**, Bar chart showing the proportion of monochromatic regions within plaques which occupy the plaque cap only (dark gray), core only (light gray) or both the core and cap (black). Data is shown for high density (10x 1 mg), low density-labeled (1x 1 mg) or all animals at the left, and stratified according to vascular regions on the right. Arch: aortic arch, DA: descending aorta, CA: carotid artery.



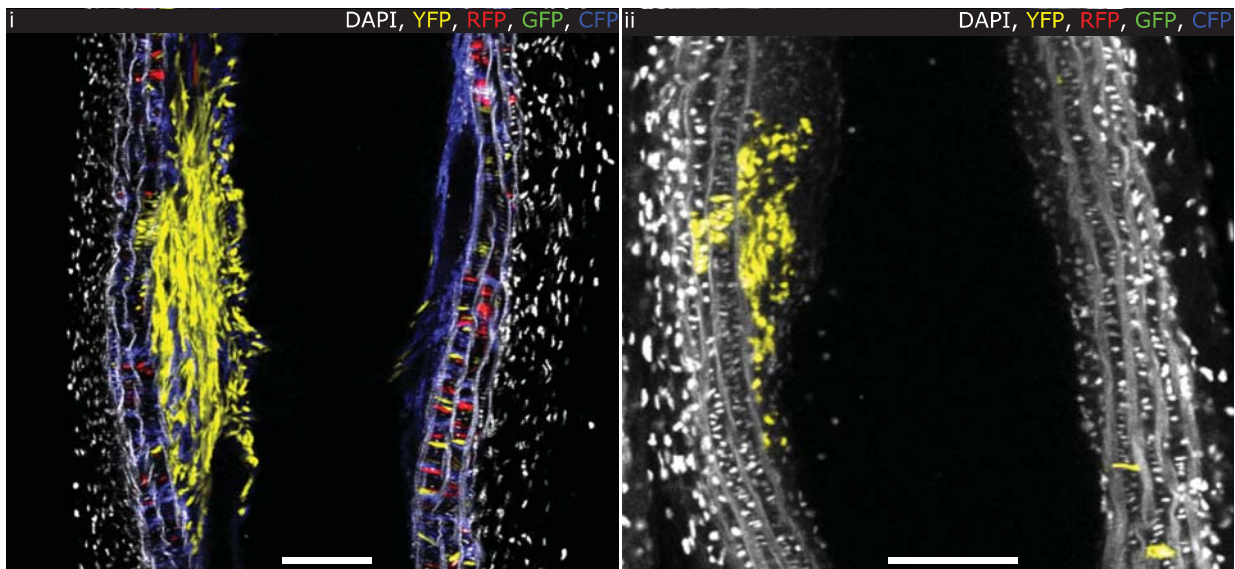
**Online Figure X: Right carotid artery immunostaining controls**

**A-D**, Single confocal scans from Z-stacks of 14  $\mu\text{m}$  cryosections from the control right carotid artery of high density-labeled (10x 1 mg tamoxifen) animal 28 days after ligation of the left carotid artery stained for aSma (**A**), Mac-3 (**B**), Smmhc/Myh11 (**C**) or EdU (**D**). For each staining, (ii-iv) are zoomed images of the regions outlined in (i). Signals for fluorescent proteins, DAPI (white), aSma (magenta), Mac3 (magenta), EdU (magenta), and Smmhc (magenta) are shown as indicated on each image. Scale bars are 50 $\mu\text{m}$ .



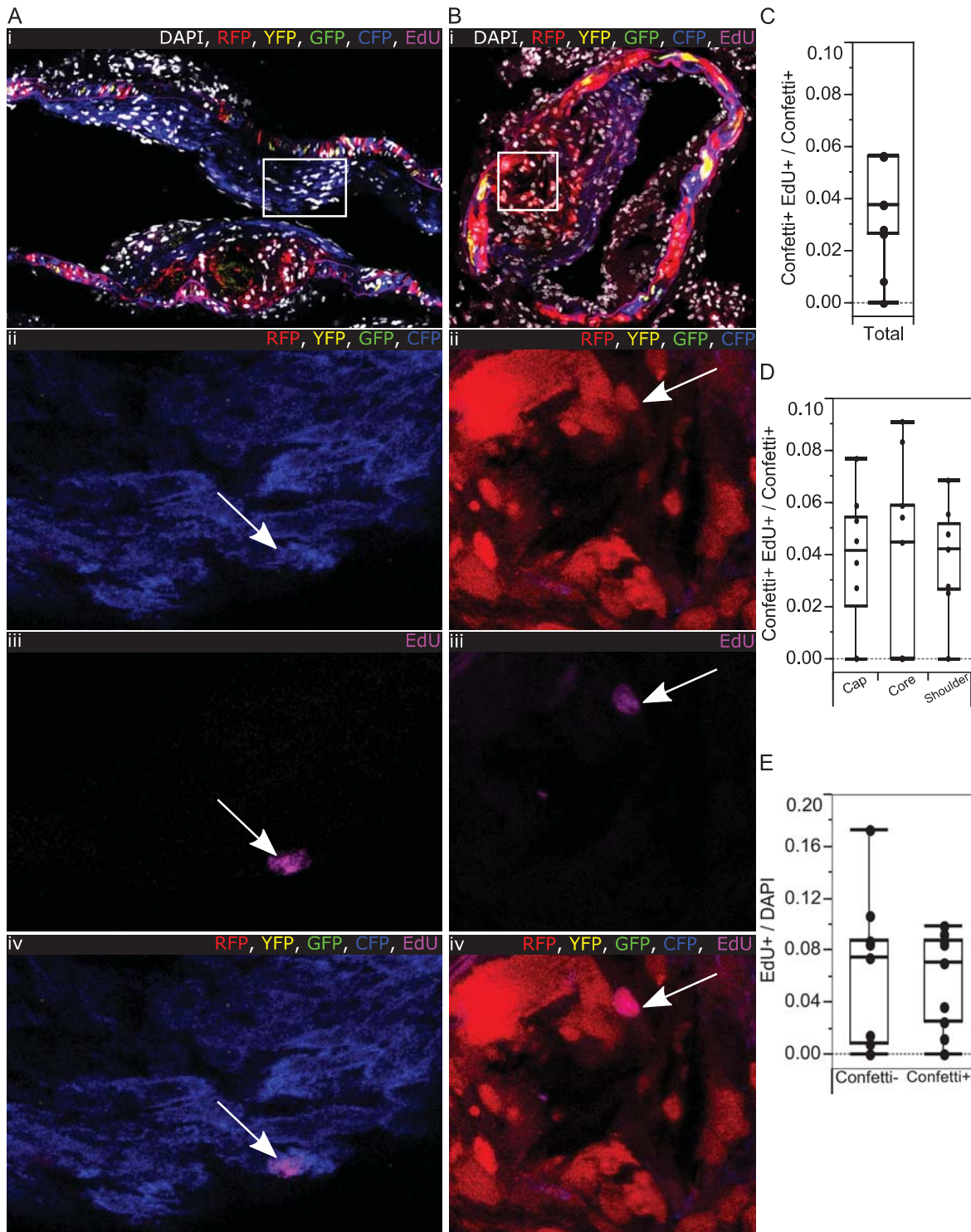
**Online Figure XI: Smmhc and EdU staining in carotid ligation-induced neointima**

**A, B,** Single confocal scans from Z-stacks of 14  $\mu$ m cryosections from the left carotid artery 28 days post-ligation in a high density-labeled animal (10x 1 mg tamoxifen) stained for Smmhc (**A**) or EdU (**B**). For each staining, the region outlined in (i) is magnified in (ii-iv). Arrows point to cells co-expressing the Confetti reporter and Smmhc (**A**) or EdU (**B**), whereas arrow heads point to cells that express the Confetti reporter, but do not stain for the respective marker. Signals for fluorescent proteins, DAPI (white), Smmhc (magenta) and EdU (magenta) are shown as indicated on each image. Scale bars are 50  $\mu$ m.



**Online Figure XII: Clonal patches span both media and neointima**

Longitudinal cross section of the left carotid artery from animals labeled at high density (10x 1 mg tamoxifen, **i**) or low density (1x 0.1 mg tamoxifen, **ii**), which were analyzed 28 days post-surgery, showing that individual VSMC-derived clones are “anchored” in the medial layer. A single scan of a confocal Z-stack, which intersects the middle of the vessel, is shown. Signals for fluorescent proteins and DAPI (white) are shown. Scale bars are 100  $\mu\text{m}$ .



**Online Figure XIII: Proliferative VSMC-derived cells detected within both the core and cap of atherosclerotic plaques**

**A, B**, Cryosections of atherosclerotic plaques from Confetti animals subjected to 16 weeks of high fat diet and injected with EdU 2 hours before analysis. The regions outlined in (i) are magnified in (ii-iv). Arrows point to EdU-positive cells expressing the Confetti reporter in the cap (**A**) or core region (**B**). Signals for fluorescent proteins, DAPI (white) and EdU (magenta) are shown as indicated on each image. **C, D**, Box plot showing the proportion of cells expressing the Confetti reporter (Confetti+) which are EdU+ (Confetti+ EdU+) displayed for all areas analyzed (**C**) and separately for the plaque cap, core and shoulder regions (**D**). **E**, Box plot showing the proportion of all cells (DAPI) which are EdU+. Data in (**C-E**) is from 7 plaques from 6 animals. All data is from high density-labeled animals.